Ensemble calculations for the atmospheric dispersion of radionuclides. Hypothetical accident scenarios in Europe: the REM case studies

de Vries, Hans; Geertsema, Gertie; Korsakissok, Irène ; Leadbetter, Susan ; Périllat, Raphaël; Scheele, Rinus ; Thomas, Jasper; Andronopoulos, Spyros; Astrup, Poul; Bedwell, Peter

Total number of authors:
18

Published in:
Guidelines for the use of ensemble calculations in an operational context, indicators to assess the quality of uncertainty modelling and ensemble calculations, and tools for ensemble calculation in emergency response

Publication date:
2019

Document Version
Publisher's PDF, also known as Version of record

D9.5.1 – Ensemble calculations for the atmospheric dispersion of radionuclides. Hypothetical accident scenarios in Europe: the REM case studies

Lead Authors: Hans De Vries, Gertie Geertsema, Irène Korsakissok, Susan Leadbetter, Raphaël Périllat, Rinus Scheele, Jasper Tomas

Based on calculations from: Spyros Andronopoulos, Poul Astrup, Peter Bedwell, Tom Charnock, Thomas Hamburger, Ievgen Ievdin, Susan Leadbetter, Tamás Pázmándi, Raphaël Périllat, Csilla Rudas, Andrey Sogachev, Péter Szántó, Joseph Wellings

Review(s): Peter Bedwell, Susan Leadbetter, Spyros Andronopoulos, Jasper Tomas, Csilla Rudas, Gertie Geertsema

Table of Contents

Introduction

One of the aims of the CONFIDENCE project is to understand, reduce and cope with the uncertainty of meteorological and radiological data and their further propagation in decision support systems, including atmospheric dispersion, dose estimation, food-chain modelling and countermeasure simulation models. Work package 1 (WP1) is focused on the modelling of uncertainties during the emergency phase, from meteorological and source term inputs, and applied to atmospheric dispersion and dose estimates. This report presents ensemble dispersion simulations performed by WP1 participants for hypothetical accident scenarios at the nuclear power plant (NPP) in Borssele (The Netherlands). These case studies are called the REM (Radiological Ensemble Modelling) scenarios.

The first part of the report summarizes briefly the two release scenarios (one short and one long release) and the two meteorological scenarios (one with small variability, one with larger variability) considered. Then, the following parts present the results for the different case studies.

Description of the REM case studies scenarios

In Figure 1 the location of the Borssele nuclear power plant (NPP) is shown. It is located at a latitude and longitude of 51.43 and 3.71 decimal degrees, respectively.

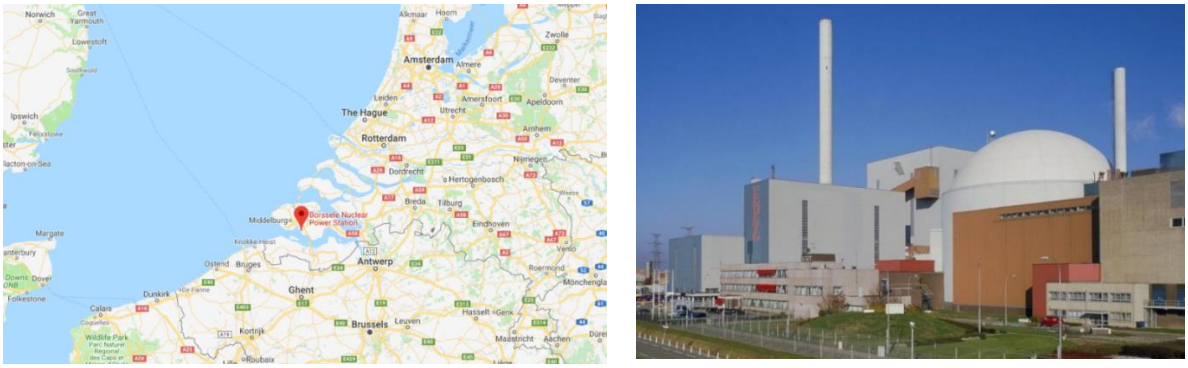

Figure 1: The Borssele nuclear power plant. Latitude, longitude: 51.43°, 3.71°

Meteorology

The meteorological data was provided by KNMI for the REM case study. The Harmonie-AROME model was used (Bengtsson et al. 2017). KNMI runs an operational and a semi-operational suite with different model versions using a Lambert Conformal coordinate system, with a horizontal resolution of 2.5 km. and a temporal resolution of one hour. The time-span of the data is 72 hours. The domain provided contained 300 x 300 points in the horizontal directions covering the area indicated by the black dots in Figure 2. The data contained 65 levels in the vertical direction up to a pressure level of 10 hPa corresponding to a height of approximately 31 km.

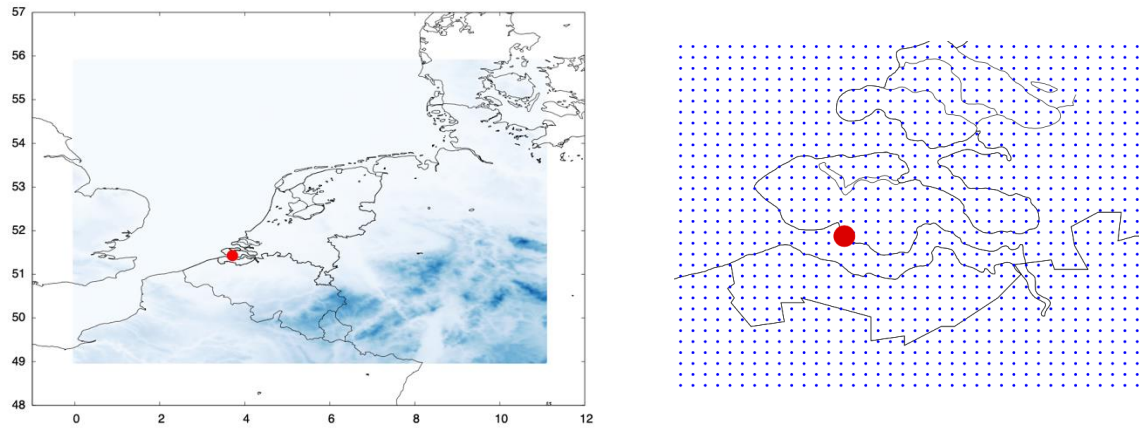

Figure 2: Meteorological domain for the REM case study. Blue dots show the horizontal resolution. Red dot indicates the location of the Borssele NPP.

KNMI constructed a Harmonie-AROME ensemble from 2 different versions of the meteorological model, with different turbulent schemes, and combined successive deterministic forecasts to create a hybrid lagged ensemble (Geertsema et al. 2019). The ensemble is hybrid in the sense that two different model versions are used; and lagged in the sense that successive forecasts are used. The reason to construct an ensemble in this way is that the KNMI Harmonie-AROME archive can be used to construct an ensemble where the spread of the resulting ensemble can represent a realistic ensemble spread and be used as a pilot for high resolution ensembles which start to become available. Each model version was used to construct 5 ensemble members with a forecast length of the required forecast length (Figure 3).

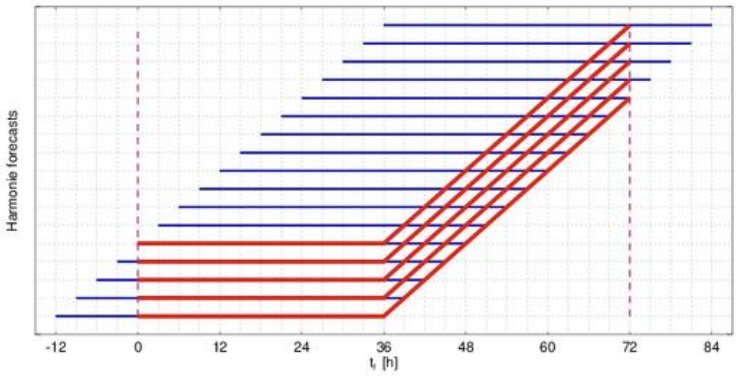

Figure 3 : Construction of a 5-member ensemble with a length of 72h. The blue lines indicate the original Harmonie-AROME 48h forecasts. The red lines indicate how each of the members is constructed.

From the start of the constructed ensemble (t_f=0), we use the forecast that starts there, and also the 4 forecasts that each started 3 hours earlier, for the first 36 hours for which they all overlap. From there, we use forecasts from successive runs to a maximum forecast of 72 hours for scenario 1 and 60 hours for scenario 2 (see below). Eventually, for all of the (hourly) steps, the date/time/forecast step values are changed to give 5 members that range from t_f=0–72 (resp. 60) for the same start date/time.

Meteorological scenario 1: “easy case”

The first scenario considered applies to a release on 11 Jan 2017. It was labelled “easy case” or “REM1”, in the sense that the wind direction is well established (Figure 4). It is an interesting case in the sense that there is rain, which adds uncertainty to the scenario (depending on the release time, the plume may or may not be scavenged by rain). Trajectories starting at Borssele at different time steps provide an indication of the plume direction (Figure 4). The trajectory calculations are based on analysed weather only.

Therefore the trajectory results provided here are only meant as indicative information. The plots show the trajectories for locations at and near Borssele, starting at different heights ranging from 10m to 500m above surface (stack height is 60 meters). The calculation length for the trajectory is 6 hours.

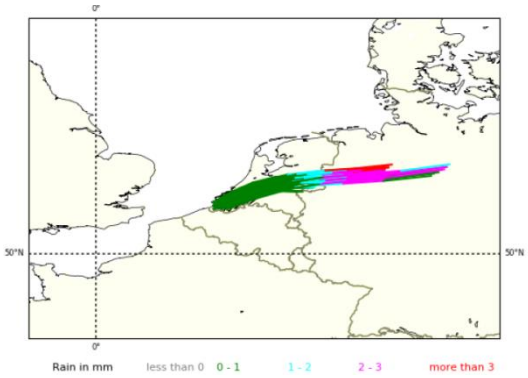

(a) Release at 06:00 UTC

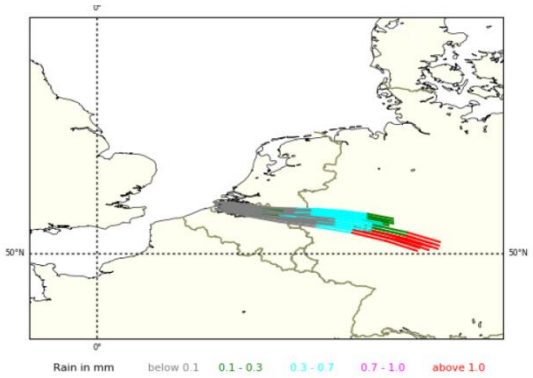

(b) Release at 12:00 UTC

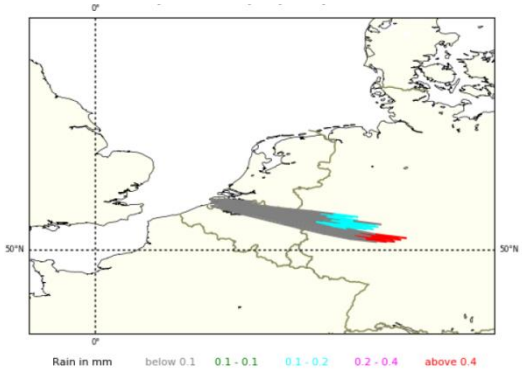

(c) Release at 18:00 UTC

Figure 4 : Indicative 6-hours plume trajectories based on analysed weather as a function of height (between 10m and 500m), for a release on 11/01/17 at 06:00, 12:00 and 18:00 UTC, and associated rain cumulated on one hour (colours show the amount of rain. Trajectories plotted by KNMI.

Figure 4 indicates that the wind direction is and clearly shifting to more northerly through the course of the day, but with little uncertainty when considering a short release at 12:00 UTC. However, these are trajectories based on the analysed weather only, and it is interesting to have a look on the trajectories given by the ensemble, in order to infer the spread featured by the different members. For further analysis, trajectories were plotted for the 10 ensemble members, for a release of particles between ground level and 100 meters above ground level, and at 12:00UTC (Figure 5). This tends to confirm that for this case, there is little uncertainty in the wind direction. However, on full ensemble dispersion simulations, the effect of rain on the plume deposition may lead to a little more variability between the ensemble members.

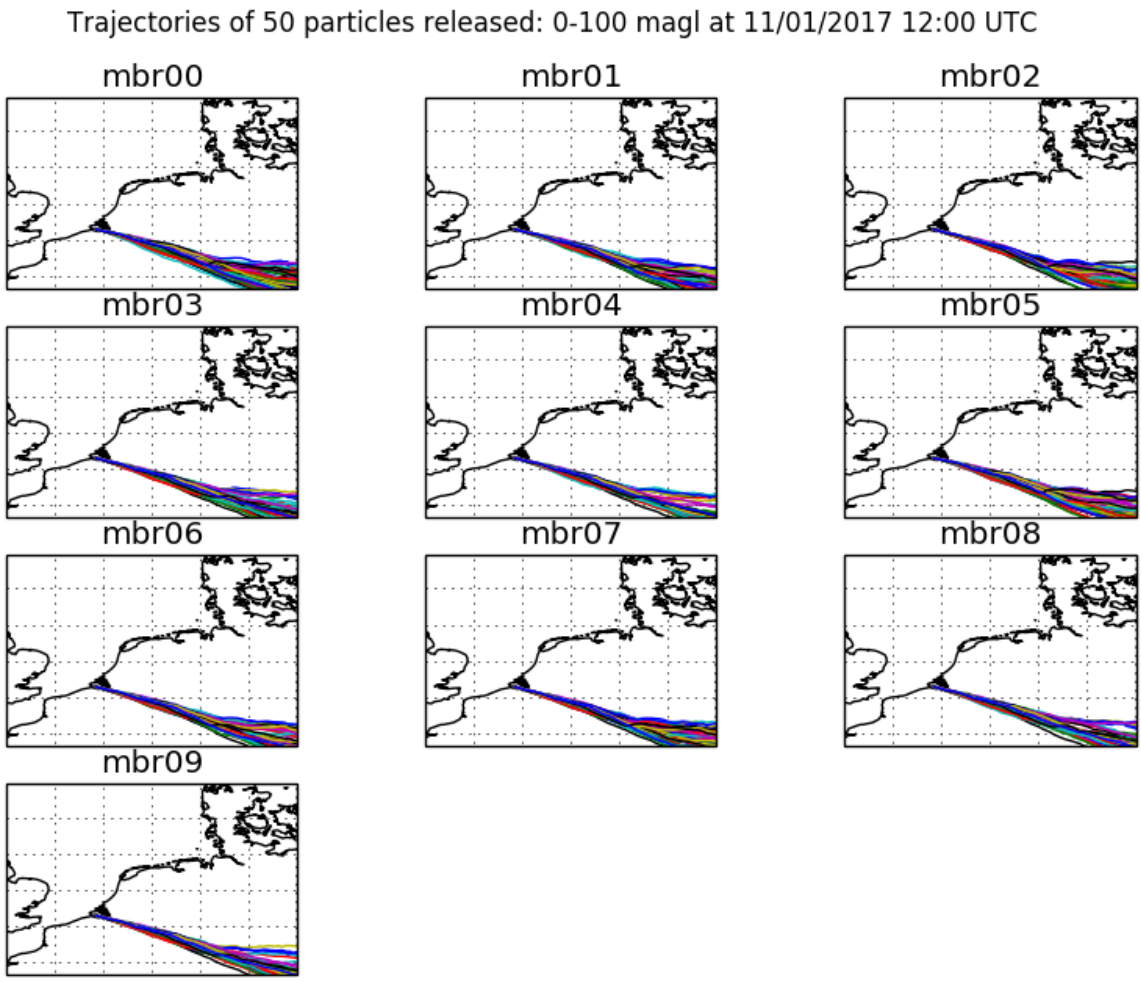

Figure 5 : trajectories for the 10 ensemble members for a release on 11 January 2017 at 12:00 UTC. Trajectories plotted by MetOffice.

Meteorological scenario 2: "warm front, higher variability case"

The second scenario considered is a weather situation with a warm front passage resulting in precipitation, wind direction and wind speed changes. It occurs on the day following scenario 1, that is, for a release on January 12, 2017.The trajectories are shown in Figure 6. The length of the trajectories is 6 hours. The colour codes denote the amount of precipitation. The trajectories start at different heights between 10 and 500 metres above surface. The trajectories start at the Borssele site and 8 locations close to the Borssele site, thus mimicking a (small) timing error in the model. The trajectories starting at 12 UTC move slowly to the North East, while the moving warm front catches up with the plume resulting in significant amount of precipitation (pink and red colours close to the release site). Trajectories starting at 18 UTC move faster to the East with precipitation close to the source. It was labelled "warm front – higher variability case" or "REM2".

The wind information from KNMI observations sites in the vicinity of the Borssele site is analysed. Three observation sites are within approximately 40 kilometres of the plant (stations 308, 310 and 340 in Figure 7). Meteorological information from three other sites located North-North East of the plant are also analysed. These 6 stations show the passage of the warm front over the area. The wind observations shown in Figure 7 clearly feature the warm front passage between 18:00 and 21:00 UTC on January 12, resulting in a change of wind speed and wind direction.

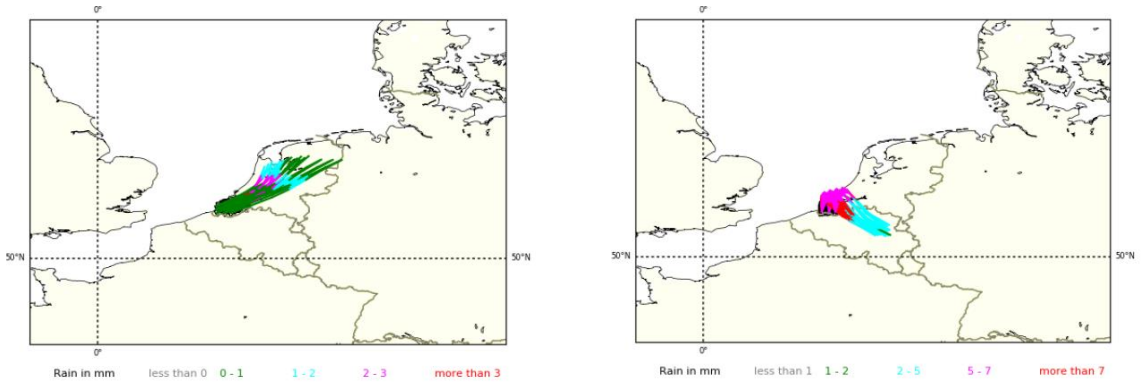

(a) Release at 12:00 UTC

(b) Release at 18:00 UTC

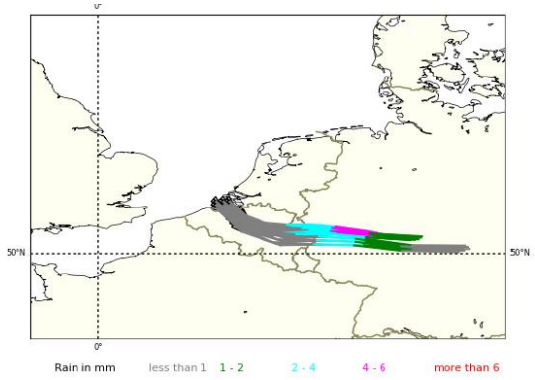

(c) Release on 13 Jan 2017 at 00:00 UTC

Figure 6 : Indicative 6-hours plume trajectories based on analysed weather as a function of height (between 10m and 500m), for a release on 12/01/17 at 12:00, 18:00 UTC, and 13/01/17 at 00:00 UTC and rain (cumulated in one hour). Trajectories plotted by KNMI.

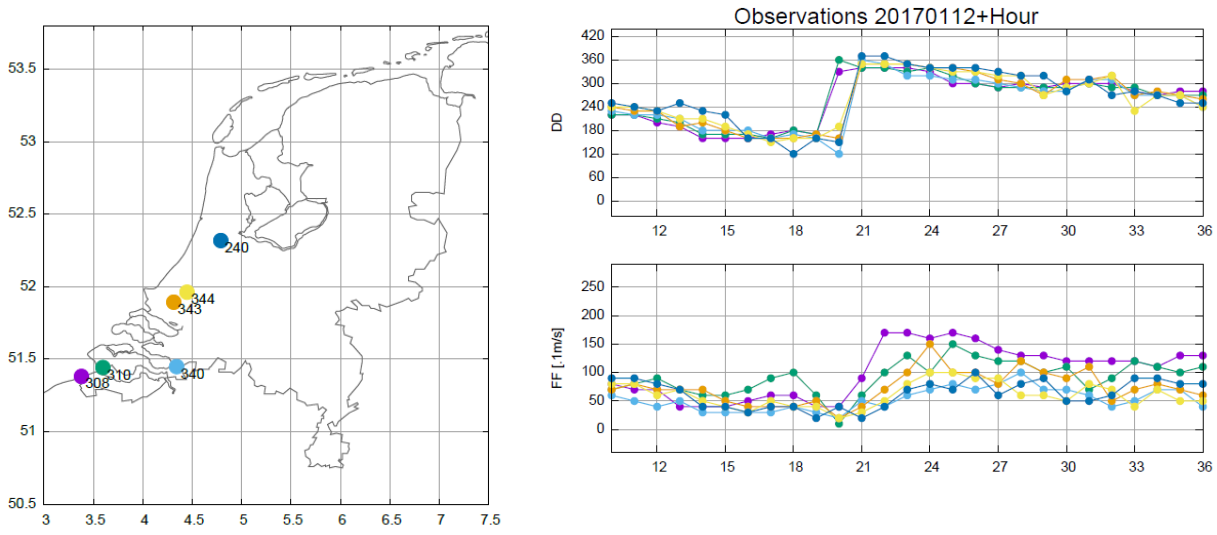

Figure 7 : Meteorological observations: position of the stations (left), wind direction (upper right) and wind speed at 10 m (lower right) averaged over previous 10 minutes, between T0=20170112 and T0+36 hours . The wind direction is given in meteorological convention (360=North, 90=East, 180=South 270=West). The colour code of the stations corresponds to the colours used on the right panel. The observations are from the KNMI archive.

As for the “easy case”, it is interesting to investigate whether the constructed ensemble features some variability in variables such as wind direction, wind speed, and rain, and how that variability translates into different plume trajectories. To answer the first question, meteograms were plotted (Figure 8). The ensemble spread is not very large during the first 36 hours (corresponding to the “easy case” described

earlier), but the variability increases after the passage of the warm front. This is particularly true for the 250-m wind speed and direction. There is also some variability in the rain.

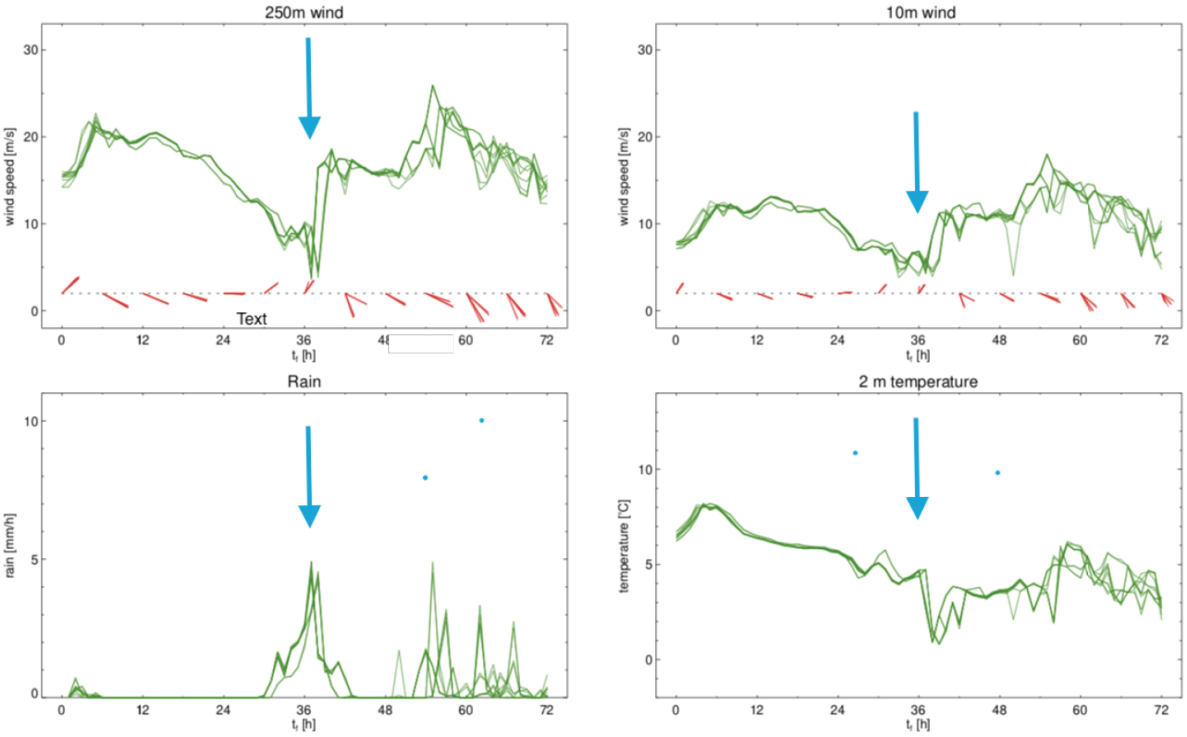

Figure 8 Harmonie ensemble meteogram. Analysis time is 2017011106. The blue arrows indicate the warm front passage, which is at 20170112 at 18:00 UTC (36 hours forecast). The green lines are the ensemble members, for 250-m and 10-m wind speed (upper left and right respectively), rain (lower left) and 2-m temperature (lower right). The red lines feature the wind direction (upper panel) at 250-m (left) and 10-m height (right). Meteograms from KNMI.

Finally, Figure 9 features the trajectories for the 10 ensemble members, for a release on 12 January 2017 at 18:00UTC. Here, there is more variability in plume trajectories than in Figure 5: some ensemble members feature trajectories toward North-North-East (e.g. members 02, 07) while others have completely shifted toward East-South-East (e.g. members 04 and 09). Some members show a turning wind during this period, with a few trajectories going in the Northern direction and most oriented toward the Southern direction (members 00, 01, 06). One may expect that the inclusion of rain in the full dispersion calculations may add further variability to the results.

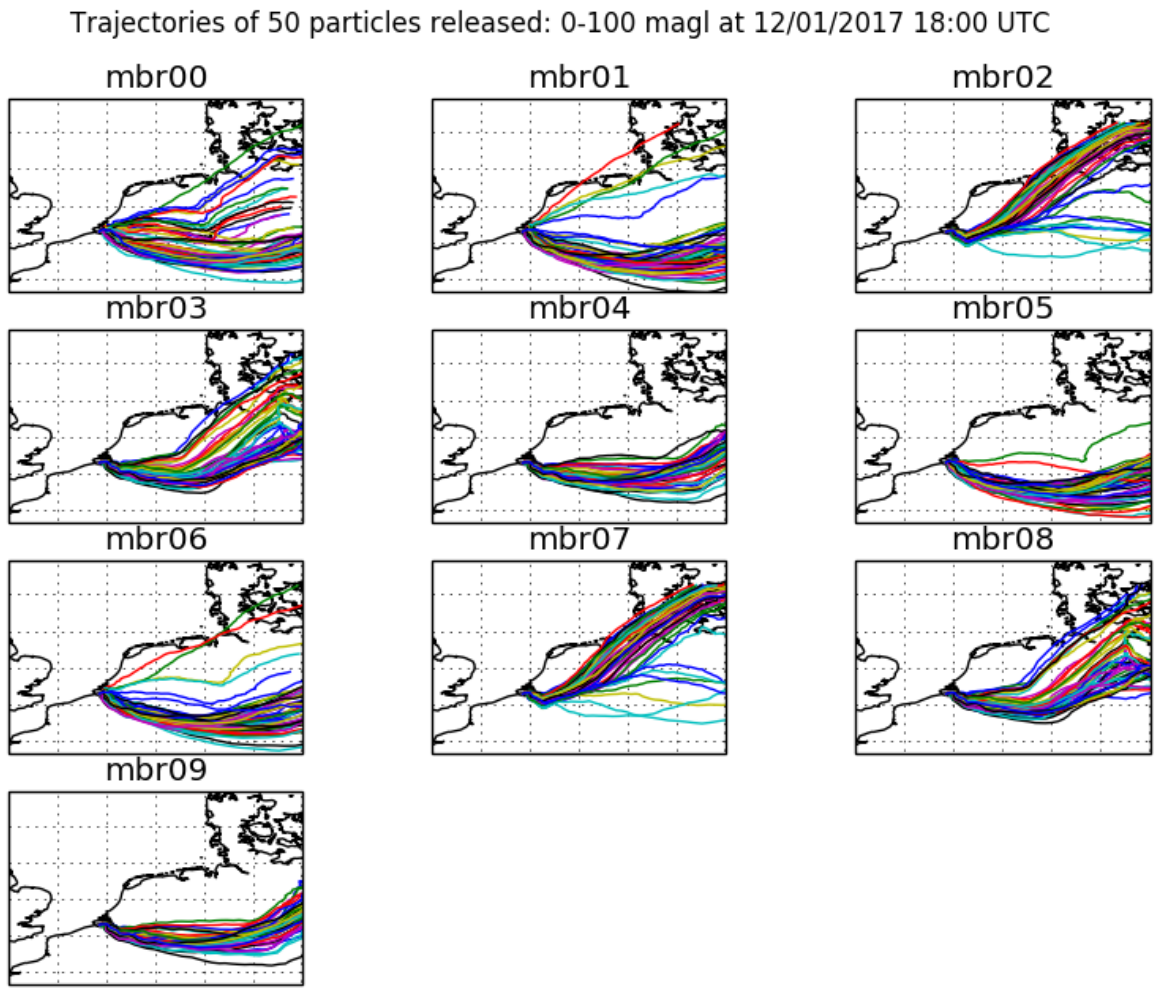

Figure 9 : trajectories for the 10 ensemble members for a release on 12 January 2017 at18:00 UTC. Trajectories plotted by MetOffice.

Release scenarios and associated uncertainties

Figure 10 schematically shows the timeline and the names of the events during an incident at a nuclear reactor involving a release of radioactivity. The horizontal arrows indicate the duration of the events and their dependencies. The variable positions of the events represent the uncertainties in their timing. Clearly, these uncertainties can complicate the assessment of the situation. As time passes, uncertainties may decrease due to additional information about the status of the reactor or through measurements.

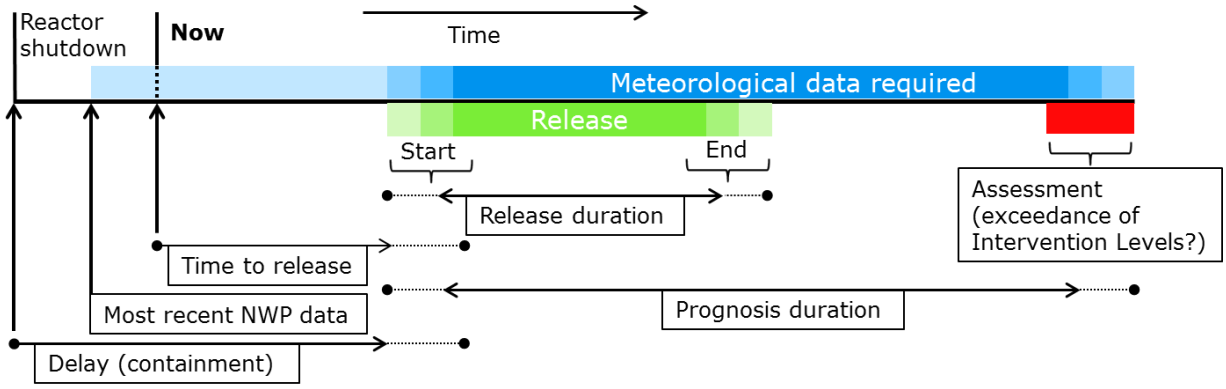

Figure 10: Illustrative timeline with the events during an incident at a nuclear reactor involving a release of radioactivity including uncertainties.

The pre-release and release phase are studied by considering two hypothetical release scenarios:

1. A release with duration of 4 hours; this is based on an accident which is anticipated to start in approximately 24 hours;
2. A release with duration of three days based on a 'Loss of Coolant Accident' (LOCA) scenario from the FASTNET project. There is no uncertainty on the timing of the start of the release. This scenario is representative of the uncertainties during the release phase (see Fig. 10). The construction of this ensemble of source terms was detailed in CONFIDENCE deliverable D9.1 (Mathieu et al. 2018).

Table 1: uncertainties considered in the two release scenarios: short release and long release

Short release	Long release
Time to release: 24 h +/- 6 h, equally distributed **Release duration**: 4 hours **Effective release height:** 50 m +/- 50 m, equally distributed **Released activity** : Factor 1/3 to 3 of Table 2	**Time to release**: 0 hours, no uncertainties **Release duration**: 3 days **Effective release height**: 50 m +/- 50 m, equally distributed **Released activity**: given by the spread of the ensemble of source terms

In Table 1 the source terms and associated uncertainties are summarized; the timing, release height and the released activity are shown for the two scenarios. The rationale behind these two source terms is that the "short release" is a very preliminary estimate, when little information is available in the pre-release phase, and the uncertainty on the release time is large. The long release is representative of uncertainties that stem from models used to represent reactors physics during severe accidents, when the accident scenario is known and there is no uncertainty on the release time (during the release phase for instance). These two source terms therefore represent different situations in emergency response. For example, the approximate time to release of 24 hours in the short release scenario might allow for direct countermeasures in the pre-release phase, such as evacuation and/or iodine prophylaxis, even though source term uncertainties are large. In the long release scenario, on the other hand, the release start now and depending on the onset of the scenario direct countermeasures might have been initiated already.

Details on the release scenarios

The nuclide composition for the short release is based on a constructed source term derived through interpolation of results from a safety study of the Borssele NPP. This source term is scaled to a hypothetical reactor with an electrical power output of 900 MW (to be consistent with the reactor considered in the long release scenario). For the short release the nuclide composition is based on a *Delay* time of 24 h. In addition, the uncertainty in the released activity is assumed to be within a factor of 1/3 to 3 of the reference values in Table 2. For the long release the uncertainty in the released activity was derived from the distribution of the source terms in the FASTNET project (Chevalier-Jabet 2019a). The median and maximum values are shown in the table for the same radionuclides as for the short release. However, the full source terms included over 200 radionuclides in total. The FASTNET ensemble of source terms was constructed using the severe accident code ASTEC, and several assumptions as inputs for the LOCA scenario. For instance, a 3-inches break was assumed, with an uncertainty of +/- 1 inch on the break size. In the same way, other uncertainties were taken into account, including the release rate (factor 10), leak rate (factor 2), iodine behaviour and concrete-corium interaction (10% error). These uncertainties were detailed in Mathieu et al. (2018) and Chevalier-Jabet (2019b). It resulted in an ensemble of 150 source terms for a three-day release. The particularity of the release kinetics is that, after the initial release start, there is a second, more important release, corresponding to the opening of the filtered venting containment system. For this second release, aerosols are supposed to be filtered but there is an important release of gaseous materials, in particular Iodine and Xenon, which explains why the released amounts for these radionuclides is much larger than, for instance, for Caesium (Table 2).

Table 2: The nuclide composition of the hypothetical source terms for the REM case study. The total released activity is shown for all nuclides in the source term. Only the eight nuclides in bold font were considered in the model runs.

	Short release	**Long release**
	Borssele NPP scaled to 900 MWe: Total released activity [Bq]	*FASTNET 3 inches break:* Total released activity [Bq] median (max)
	Particle size: 1 µm. Iodine group: 1/3 particulate, 2/3 elemental	Iodine form: given by the ensemble of source terms
Nuclide		
Kr-85m	8.76E+15	6.65E+15 (2.89E+16)
Kr-85	1.53E+16	2.08E+16 (2.12E+16)
Kr-88	2.38E+15	2.36E+15 (1.62E+16)
Xe-133	**3.51E+18**	**4.97E+18 (5.25E+18)**
Xe-135	7.46E+17	8.99E+17 (1.64E+18)
I-131	**2.25E+16**	**1.08E+15 (1.972E+16)**
I-132	**2.84E+16**	**1.23E+15 (2.21E+16)**
I-133	2.15E+16	6.62E+14 (1.21E+16)
I-135	3.04E+15	6.47E+13 (1.19E+15)
Rb-88	1.97E+13	2.83E+13 (7.32E+13)
Sr-89	2.36E+15	3.46E+12 (2.89E+13)
Sr-90	2.19E+14	2.36E+11 (1.97E+12)
Y-90	1.78E+13	5.91E+09 (1.60E+11)
Zr-95	4.19E+14	1.33E+10 (4.40E+12)
Ru-103	3.80E+15	1.79E+13 (1.31E+14)
Ru-106	1.24E+15	6.71E+12 (4.93E+13)
Rh-106	1.24E+15	6.67E+14 (1.33E+18)
Te-131m	1.02E+15	8.51E+12 (3.05E+13)
Te-132	**1.37E+16**	**6.58E+13 (2.41E+14)**
Cs-134	**2.69E+15**	**1.30E+13 (6.02E+13)**
Cs-136	**6.37E+14**	**4.90E+12 (2.22E+13)**
Cs-137	**2.06E+15**	**8.80E+12 (4.06E+13)**
Ba-137m	**2.78E+14**	**1.37E+13 (8.45E+13)**
Ba-140	4.08E+15	8.46E+13 (8.30E+14)
La-140	4.47E+14	7.67E+12 (7.04E+13)
Pu-238	2.60E+11	1.65E+08 (4.97E+10)
Pu-241	3.19E+13	5.13E+09 (1.55E+12)
Cm-242	9.02E+12	1.82E+09 (5.98E+11)
Cm-244	1.02E+11	1.43E+08 (4.68E+10)

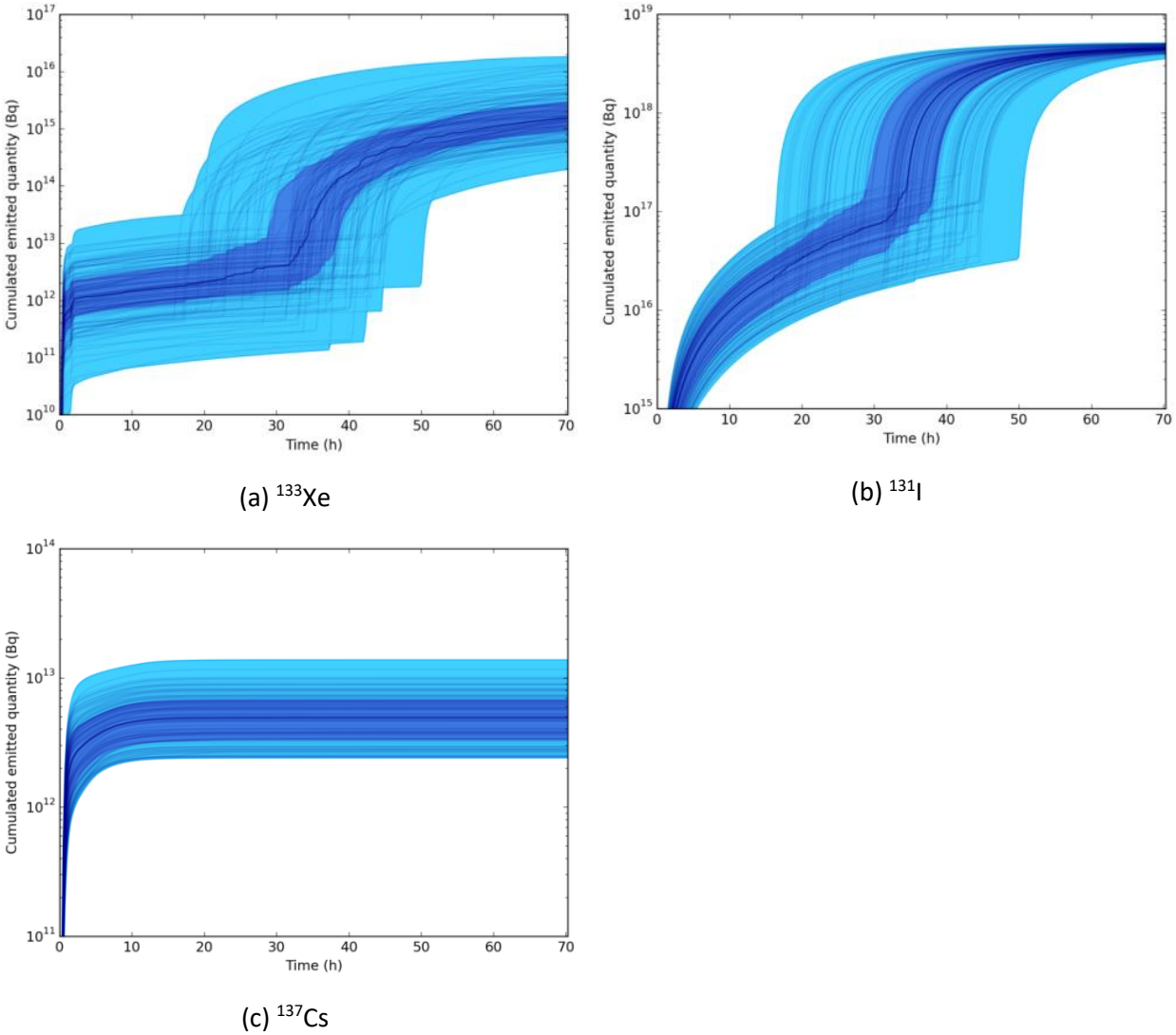

Figure 11 : release kinetics for the long release ensemble from the FASTNET project, for three radionuclides.

It should be noted that several simplifications have been made in this study for the sake of computational time. First, for the short release as well as the long release scenarios, only the eight radionuclides highlighted in bold in Table 2 have been used. This selection comes from previous Fukushima studies. Those were radionuclides considered having a significant contribution to the dose (Saunier et al. 2013). However, several significant contributors have been overlooked, especially Tellurium and, as far as agricultural contamination is concerned, ^{90}Sr for instance.

The second approximation was made for the long release scenario. The full ensemble of 150 source terms was not used. Two subsets of 5 and 10 source terms have been defined, in order to keep some properties of the ensemble (mean and standard deviation). The method used is detailed in (Bedwell et al. 2019). Most participants have used the 10 source terms for their long release calculations, except DTU and MTA EK who used the 5 source terms.

The impact of these two assumptions (reduction of the number of radionuclides and reduction of the number of ensemble members) was assessed by comparison to “full” calculations. This is presented in Bedwell et al. (2019).

Atmospheric dispersion simulations setup and endpoints

Table 3 summarizes the two different meteorological scenarios and two release scenarios that have been described. The short release scenario was used with both meteorological scenarios REM1 and REM2. Therefore, the corresponding case studies will be labelled hereafter as REM1 (or REM2)-short release or REM1-S (REM2-S) as summarized in Table 3. The long release scenario was used with the meteorological data provided for REM1 study; however, as the release lasts three days, it covers both REM1 and REM2 meteorological situations. The case study will therefore be named REM-long release or, to be concise, REM-L.

Table 3 : Synthesis of the meteorological and release scenarios, and corresponding short names of the case studies

Case studies	Short release	Long release (FASTNET release)
Meteorological scenario 1 (easy case) - REM1	REM1-S	REM-L
Meteorological scenario 2 (warm front) - REM2	REM2-S	

Modelling set-up

Table 4 summarizes the participants who ran simulations for the REM case study and the endpoints that were computed by the participants. It also presents the type of atmospheric dispersion model used: one Eulerian model, one Lagrangian particle model, one Lagrangian puff model and four Gaussian puff models.

Table 4 : Summary of participants, output variables computed, and type of atmospheric dispersion model. The green cells indicate the outputs provided by participants. The white cells correspond to outputs reconstructed by IRSN using activity, deposition, and IRSN's assumptions for dose calculation.

		Activity	Deposition	Dose rate	Dose	Type of model
France	**IRSN**	✓	✓	✓	✓	IdX – Eulerian
The Netherlands	**RIVM**	✓	✓	✓	✓	NPK-puff – Gaussian puff
Germany	**BfS**	✓	✓	✓	✓	RIMPUFF – Gaussian puff
UK	**Met Office/PHE**	✓	✓		✓	NAME – Lagrangian particle
Greece	**EEAE**	✓	✓	✓		DIPCOT – Lagrangian puff
Denmark	**DTU**	✓	✓			RIMPUFF – Gaussian puff
Hungary	**MTA EK**	✓	✓	✓	✓	SINAC – Gaussian puff

Apart from the type of model that differs from one participant to another, discrepancies in the outputs may stem from various physical parameterizations, notably those related to dry and wet deposition (Bedwell et al. 2018). Considering the importance of precipitation in the two meteorological scenarios considered, it is worth studying the difference in wet deposition schemes between the participants (Table 5). For most models, scavenging coefficients are of the form $\Lambda = aq^b$ where q is the rain intensity (mm.h^{-1}) and Λ is in s^{-1}. Factors a and b are given by the user and may depend on the height, with a distinction mixing layer / reservoir layer (RIVM), in-cloud or below cloud scavenging

(which is diagnosed through computing the cloud basis height) (IRSN and MetOffice), and/or on isotope families (DTU). For particles, the models used by EEAE and BfS compute the scavenging coefficient as function of the particle size and the rain intensity according to Baklanov and Sørensen (2001). The washout coefficient $\Lambda(s^{-1})$ is expressed as a polynomial function of particle radius *r* (µm) and rain-rate *q* (mm/h) as follows:

$$\begin{array}{cc} \Lambda(r,q) = a_0 q^{0.79} & r < 1.4\mu m \\ \Lambda(r,q) = (b_0 + b_1 r + b_2 r^2 + b_3 r^3) f(q) & 1.4\mu m < r < 10\mu m \\ \Lambda(r,q) = f(q) & r > 10\mu m \end{array}$$

with

$$f(q) = a_1 q + a_2 q^2$$

and

$$a_0 = 8.4 \cdot 10^{-5}, a_1 = 2.7 \cdot 10^{-4}, a_2 = -3.618 \cdot 10^{-6}$$

$$b_0 = -0.1483, b_1 = 0.3220133, b_2 = -3.0062 \cdot 10^{-2}, b_3 = 9.34458 \cdot 10^{-4}$$

For the calculations presented here, a particle size of 1µm was assumed. Therefore, the values presented in Table 5 for EEAE and BfS are given for this particle size. RIVM and IRSN have different values for in-cloud and below-cloud scavenging, but used a uniform value over the boundary layer height in this case. However, in practice, IRSN generated their ensembles using Monte Carlo perturbations for the REM1 and REM2 cases. Therefore, the reference value indicated in Table 5 was only used for the REM1-L case where simulations were compared for 10 meteorological members without additional perturbation (see REM1-S results below). For the "full" perturbations of REM1, see Table 7.

Table 5 : Scavenging coefficients used by the different participants

	Type of model	Scavenging scheme aq^b - Coefficients values	
		a ($h.mm^{-1}.s^{-1}$)	b
IRSN	ldX – Eulerian	Below cloud: $a=5\times10^{-5*}$ In cloud: $a=1\times10^{-4}$	b=1
RIVM	NPK-puff – Gaussian puff	Below cloud: $a=7.0\times10^{-5}$ In cloud: $a=7.0\times10^{-5*}$	For q < 1 mm/h, b=1, else b=0.8
BfS	RIMPUFF – Gaussian puff	Gases: $a=8\times10^{-5}$ Aerosols 1µm: $a=8.4\times10^{-5}$	Gases: b=0.6 Aerosols 1µm: b=0.79
MetOffice/PHE	NAME – Lagrangian particle	Below cloud: $a=8.4\times10^{-5}$ In cloud: $a=3.36\times10^{-4}$	b=0.79
EEAE	DIPCOT – Lagrangian puff	Gases: $a=8\times10^{-5}$ Aerosols 1µm: $a=8.4\times10^{-5}$	Gases: b=0.6 Aerosols 1µm: b=0.79
DTU	RIMPUFF – Gaussian puff	*Depends on the isotope family*	
MTA EK	SINAC – Gaussian puff	$a=1\times10^{-4}$	b=0.8

* Used in this study for all layers (no distinction between below-cloud and in-cloud)

The variability featured in Table 5 is consistent with the range of variation of an order of magnitude pointed out in Bedwell et al. (2018). However, in this study, when considering a rain rate of 1 mm/h and assuming the main process is below-cloud scavenging (which is true close to the source), the range of variation is

much lower: the scavenging coefficient Λ is within $[5\times10^{-5};8.4\times10^{-5}]s^{-1}$ with the exception of MTA-EK (1×10^{-4}). Farther from the source, when in-cloud scavenging may be included, Met Office may have higher deposition than the others with $\Lambda = 3.36\times10^{-4}s^{-1}$ for in-cloud scavenging (again, for a rain of 1 mm/h). Overall, it may be supposed that, all other things being equal, the highest deposition values should probably be obtained by Met Office and/or MTA EK.

Synthesis of the case studies

For the two short release scenarios (REM1-S and REM2-S) perturbations were applied to the "reference" release, to account for the uncertainties described in Table 1. The exact way these uncertainties should be taken into account was left to be decided by the participants, depending on their practical possibilities (especially in terms of computational resources). In practice, it resulted in between 10 and 650 simulations per release scenario, as detailed in Table 6.

Table 6 : source perturbations applied for the short release scenario, in the REM1 and REM2 case studies.

Participant	Number of simulations per release scenario	Source perturbations		
		Release height	Release time	Released quantity
IRSN	100 (Monte Carlo)	[0, 100m] uniform	[-6h, 6h] uniform	[1/3, 3] uniform
BfS	150	[0m, 50m, 100m]	T0 + [-6h, -3h, 0h, +3h, +6h]	[x1/3, x1, x3]*
Met Office/ PHE	90	[50m]	T0 + [-6h, 0h, +6h]	[x1/3, x1, x3]
EEAE	50	[50m]	T0 + [-6h, -3h, 0h, +3h, +6h]	[x1/3, x1, x3]*
MTA EK	150 (REM 1-S) 90 (REM 2-S)	[0m, 50m, 100m]	T0 + [-6h, -3h, 0h, +3h, +6h] T0 + [-6h, 0h, +6h]	[x1/3, x1, x3]*
RIVM	650	[0m, 25m, 50m, 75m, 100m]	[-6h, +6h] with a time step of 1 hour (13 steps)	[x1/3, x1, x3]*
DTU	10 (REM 1-S) 50 (REM 2-S)	[50m]	T0 + [-6h, -3h, 0h, +3h, +6h] (REM2-S)	[x1/3, x1, x3]*

*Perturbation applied a posteriori on the results

IRSN decided to apply perturbations to the model's physical parameters, namely vertical diffusion coefficients, dry deposition velocities and scavenging coefficients, to account for model uncertainties

described in (Bedwell et al. 2018). The ranges of variation for these parameters are given in Table 7. As it would not be possible to run "cross-simulations", that is, taking into account all combinations of parameters, IRSN used a Monte Carlo method, which consists of randomly drawing the uncertain parameters' values within the given range of variation; a set of N combinations is drawn, N being chosen by the user to ensure that there is sufficient convergence in the results (here, N=100). The Monte Carlo method, convergence and limitations are discussed in Bedwell et al. (2019). Besides, Périllat et al. (2017) already compared the use of "cross-simulations", using a meteorological ensemble and a set of source terms on the Fukushima case, and Monte Carlo method including the variation of physical parameters in the model. It concluded that meteorology and source terms were the main sources of uncertainties, and results were not significantly different using the "full" Monte Carlo ensembles in terms of ensemble's ability to encompass the observations. The main advantage of using Monte Carlo is reducing the number of simulations, while allowing to take into account more sources of uncertainties.

Table 7 : Perturbations applied by IRSN for the short release scenario, in the REM1 and REM2 case studies. The (x) denote a multiplicative coefficient applied to the reference value; the (+) is an additive perturbation applied to the reference value; no sign indicates that the parameter's range of variation is directly given by the table.

	Variable	Lower bound	Upper bound
Source term	Source term amplitude (×)	0.333	3
	Source term time shift (+)	- 6 H	+ 6 H
	Source term height	0 m	100 m
Model (physical parameters)	Dry deposition (iodine)	2.0×10^{-3} m/s	2.0×10^{-2} m/s
	Dry deposition (others)	5.0×10^{-4} m/s	5.0×10^{-3} m/s
	Scavenging coefficient a (in cloud)	1.0×10^{-5} h.mm^{-1}.s^{-1}	1.0×10^{-2} h.mm^{-1}.s^{-1}
	Scavenging coefficient a (below cloud)	1.0×10^{-5} h.mm^{-1}.s^{-1}	1.0×10^{-4} h.mm^{-1}.s^{-1}
	Scavenging coefficient b	0.5	1.0
	Vertical diffusion matrix Kz (×)	0.333	3

Endpoints

Some participants provided their own dose calculations (see Table 4). For those who provided only atmospheric dispersion results (air and deposition concentrations for all radionuclides), the dose calculations were made by IRSN, based on the air concentrations and deposition data provided. The dose calculations were derived for 1-year-old children, with no sheltering nor any other forms of protective action. The effective dose calculation includes the following pathways:

- External dose due to irradiation by radionuclides in the atmosphere (plume-shine),
- External dose due to the irradiation by radionuclides deposited on the ground (ground-shine),
- Internal dose due to plume inhalation.

It does not take into account dose resulting from food intake.

The outputs proposed here are maps of probability of threshold exceedance[1]. Instead of a single contour showing the impacted area (based on a single deterministic simulation), the probability maps are based on an ensemble of simulations and correspond to the probability that a given zone is contaminated above a given level. The reference levels chosen for this project are:

- 37 kBq/m^2 of Cs-137 deposition (Chernobyl reference level);
- 50 mSv inhalation thyroid dose for 1-year old child (IAEA reference level for iodine intake; IAEA (2011));
- 50 mSv effective dose for 1-year old (French reference level for evacuation).

The 555 kBq/m^2 reference level for Cs-137 deposition, initially chosen (Chernobyl reference level) is not shown since the threshold is too high and was not relevant for this case study. This is also the case for the 100 mSv effective dose (IAEA reference level for evacuation). Instead, for information, additional levels were considered:

- 10 kBq/m^2 deposition for Cs-137 and I-131;
- 10 mSv effective dose for 1-year old child;
- 10 mSv inhalation thyroid dose for 1-year old child.

Once the thresholds have been chosen, useful outputs for decision making, presented in this report, are the maximum distance and surface area affected by the threshold exceedance, and associated uncertainties. In addition, to compare several uncertainty assessments, a particular percentile may be chosen and drawn for each ensemble calculation. Once a given percentile has been chosen, it may be used for decision making in the same way as a deterministic simulation. Other outputs were already provided as examples in a previous deliverable (De Vries et al. 2019) and in conference presentations (Korsakissok et al. 2019).

Ensemble results for REM1 – short release

Results are shown for the short release, using the Harmonie-AROME ensemble of 10 members for REM1 scenario. The release time is on January 11th, 2017 at 12:00 UTC, the release height is 50 m, and the released quantities are those given in Table 2. Ensembles are presented for two configurations: (a) an unperturbed source term, therefore propagating only meteorological uncertainties, and (b) with source term perturbations as described in Table 6.

Thus, all participants have the same meteorological and, in the unperturbed case, release data. The dispersion model itself differs, as well as deposition-related data. This includes the type of model (see Table 4), the dry and wet deposition models, diffusion models (Bedwell et al. 2018), and other default hypotheses such as the initial source dilution. In addition, there may also be differences in dose calculation assumptions.

Median of the ensembles

Figure 12 shows the median of the seven ensembles for ^{137}Cs deposition at the end of the calculation. Here, there are no perturbations to the source term, and no additional perturbations to the models, in order to ensure that all participants use exactly the same inputs. Therefore, the observed differences are only due to different dispersion modelling assumptions, such as the description of the atmospheric dispersion process (Eulerian, Lagrangian particle, Lagrangian puff, Gaussian puff with different parametrizations), dry deposition schemes (dry deposition velocities fixed or calculated depending on particles properties and

[1] better referred to as “level of agreement maps”, since the uncertainties taken into account are partial and the inputs do not necessarily represent the same probability.

surface roughness), wet scavenging schemes (described in Table 5), but also modelling domain (DTU and EEAE used a smaller modelling domain than other participants) and eventual use of an interpolation scheme to map the model results to the defined grid locations. In particular, conversions between Cartesian and latitude/longitude grids may be a source of approximations. This figure illustrates that the modelling differences are far from negligible, even when using exactly the same input data and even when the same dispersion model is used (BfS and DTU). The scavenging schemes presented in Table 5 did not show significant differences between the participants and, indeed, it does not seem to be a primary source of variability. For instance, BfS and EEAE used exactly the same scheme but the deposition map of BfS shows higher values than that of EEAE. The high deposition shown by Met Office far from the source (large yellow area), however, may be explained by the in-cloud scavenging which induces larger deposition than for other participants.

The median is an example of ensemble output that can be used for decision making; however, other percentiles should be examined as well, in particular to determine the possible "worst cases". Here, for the sake of brevity, other percentiles are not shown. One can refer to De Vries et al. (2019) and Berge et al. (2019) for other example outputs.

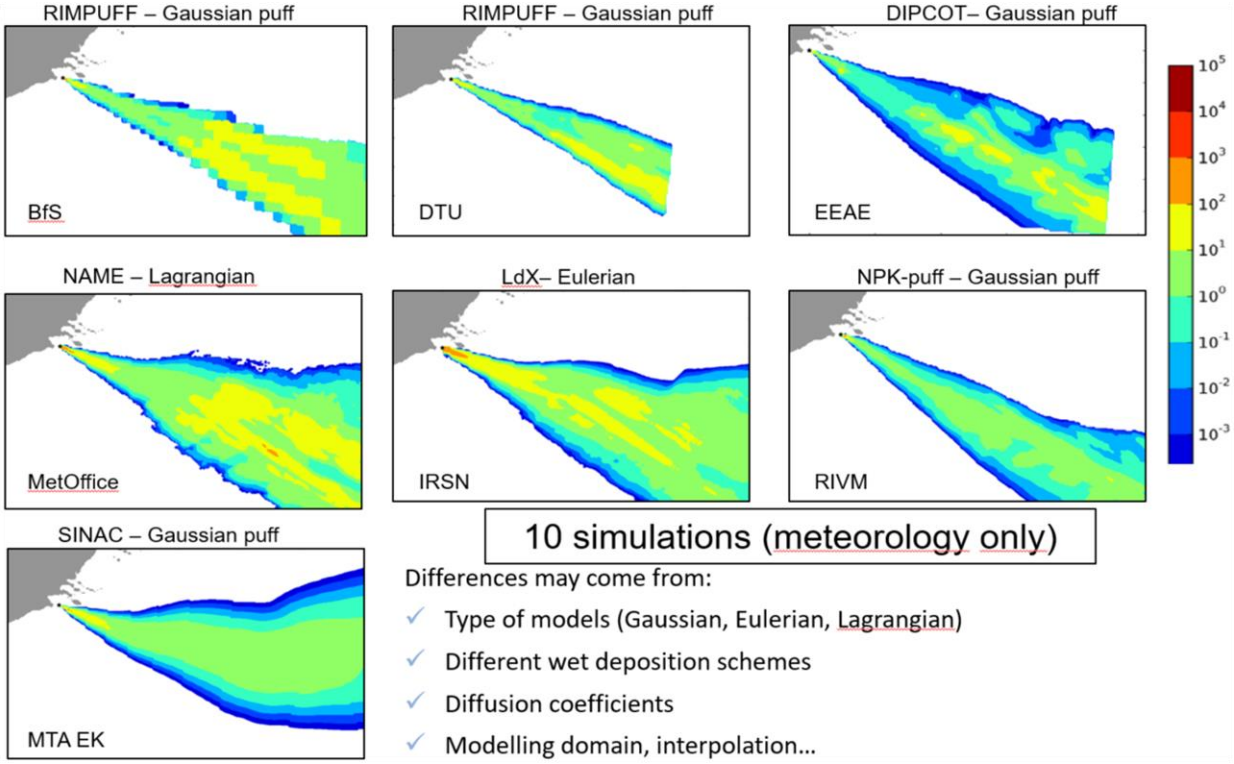

Figure 12 : median of the ^{137}Cs deposition in Bq/m^2 at the end of the release, for the seven ensembles. Only the meteorological uncertainties are taken into account (meteorological ensemble + reference source term without perturbation). Therefore, only the dispersion models differ between the participants.

Maximum distance of threshold exceedance

In Table 8, we compare the mean of the ensemble results for each participant, 24 hours after the beginning of the release. The variable of interest is the maximum distance from the source at which the threshold is exceeded, for several of the endpoints defined earlier. For each member of the ensemble, we determine the maximum distance above the given threshold (distance of the farthest grid point over the

threshold); the values given in Table 8 are the averaged values over the ensemble members (for each participant).

Table 8 : Distance (in km from the source) of the threshold exceedance averaged over the ensemble members, for the REM1 case study (short release), without source term perturbation and several variables of interest.

	Cs-137 Deposition		Inhalation thyroid dose		Effective dose	
	10 kBq/m²	37 kBq/m²	10 mSv	50 mSv	10mSv	50 mSv
BfS	543 km	447 km	142 km	40 km	16 km	4 km
DTU	417 km	403 km	97 km	37 km	11 km	0 km
EEAE	523 km	316 km	46 km	20 km	6 km	0 km
IRSN	558 km	389 km	209 km	79 km	26 km	1 km
Met Office/PHE	578 km	558 km	130 km	52 km	24 km	0 km
MTA EK	96 km	38 km	87 km	29 km	13 km	0 km
RIVM	543 km	15 km	40 km	19 km	7 km	0 km

The values of Table 8 show a high variability between the participants. This variability comes from the type of model used (see Table 4). The first two lines correspond to the same model, the Gaussian puff model RIMPUFF. However, the modelling domain is not the same, which may explain the differences in the distance reached by ^{137}Cs deposition (the end of the modelling domain is reached by several members in these simulations). Differences may also come from the assumptions made in deposition and scavenging values; for instance, Met Office has the highest distance for deposition, which may be explained by the scavenging schemes discussed previously (Table 5). EEAE used a Lagrangian puff model with an additional (to the puff grow) 3-D random motion of the puffs which maybe overestimates turbulent diffusion, leading to lower distances; differences may come from assumptions concerning the diffusion model, scavenging coefficients and dry deposition velocities. Finally, IRSN's model is Eulerian, which is known to underestimate the values near the source but gives the highest distances in this case, except for ^{137}Cs deposition. This may come from the assumptions made in computing the vertical diffusion scheme during the preprocessing step, and/or in the choice of the vertical grid resolution, both of which may lead to overestimate concentrations in the first vertical layer. The inhalation thyroid dose should not be significantly impacted by a change in deposition scheme; however, there is an additional source of variability in the assumptions made for dose calculations. Here, the variability between participants is very large. For instance, the threshold of 50 mSv (that may be used to recommend stable iodine intake in some European countries) ranges between 19 km and 79 km. In the same way, the 10 mSv threshold on effective dose ranges between 7 and 26 km.

Table 9: Distance (in km from the source) of the threshold exceedance averaged over the ensemble members, for the REM case study (short release) with source term perturbation and several variables of interest.

	Cs-137 Deposition		Inhalation thyroid dose		Effective dose	
	10 kBq/m²	37 kBq/m²	10 mSv	50 mSv	10 mSv	50 mSv
BfS	505 km	415 km	160 km	36 km	15 km	4 km
DTU	417 km	403 km	97 km	37 km	11 km	0 km
EEAE	469 km	237 km	45 km	18 km	6 km	0 km
IRSN	409 km	180 km	228 km	90km	35 km	7 km
Met Office/PHE	483 km	361 km	130 km	55 km	28 km	5 km
MTA_EK	184 km	46 km	85 km	28 km	12 km	0 km
RIVM	482 km	222 km	37 km	18 km	7 km	1 km

Maximum distances of threshold exceedance are then given for the case where source term perturbations are taken into account (Table 9). It can be noticed that the deposition distances are generally lower than those in Table 8, meaning that the source perturbations tend to decrease *on average* the deposition distance. It may be that the meteorological conditions for the perturbed release times lead to lower ground deposition (lower or no rain) than the initial release time. On the other hand, the distance for inhalation thyroid dose and effective dose thresholds tends to be similar or higher than the results without perturbation. If wet deposition is lower, then the plume is less depleted and it is consistent with a higher inhalation dose. For effective dose greater than 50 mSv, the distances were previously zero for IRSN and Met Office/PHE with the non-perturbed source term (in Table 4), while some perturbed simulations (for instance when multiplying the source term by 3) lead to non-zero distances, which explains the results in Table 9.

The previous results present an indicator useful for decision making, the "maximum distance of threshold exceedance". However, this indicator was averaged over the ensembles and did not take into account the ensembles' spreads. One of the questions is then whether the inter-model variability highlighted by these results is larger than each individual ensemble's spread. In other words, how large is the inter-model (or inter-ensemble) variability compared to the uncertainties taken into account in the ensemble simulations? Figure 13 (for the deposition) and Figure 14 (for the inhalation thyroid dose) show that the variability across the seven ensembles is typically much greater than the individual ensemble model spread given by the standard deviation, when considering the meteorological uncertainties only. This is easily explained by the fact that the meteorological uncertainty is small in this case. On the contrary, when taking into account both meteorological and source uncertainties, the ensembles' spreads are much larger, although there is still a very high variability between the medians of the seven ensembles (Figure 13(b) and Figure 14(b)). This illustrates the importance of taking into account other uncertainties besides meteorological data, including model-related uncertainties.

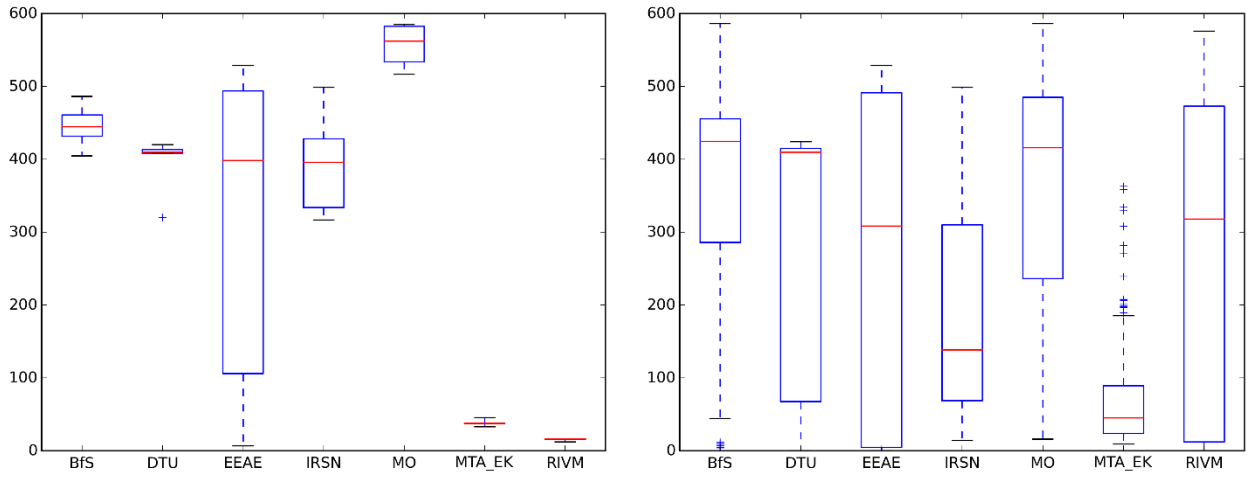

(a) Meteorological uncertainty only (b) Meteorology + ST perturbations

Figure 13: Ensemble mean of the maximum distance (in km) for the threshold exceedance of 37 kBq/m² of ^{137}Cs deposition for the seven participants, 24 hours after the beginning of the release, and associated standard deviations.

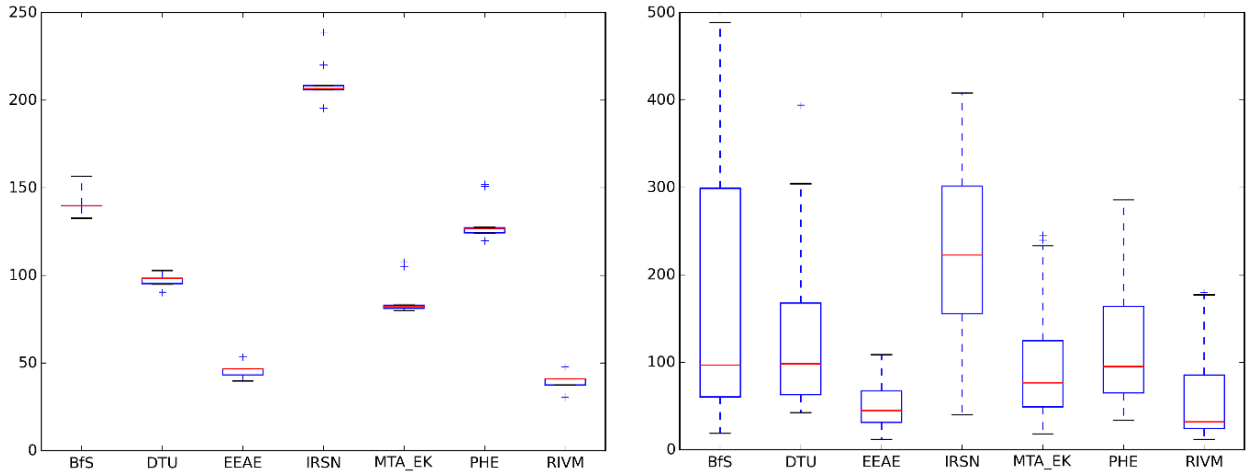

(a) Meteorological uncertainty only (b) Meteorology + ST perturbations

Figure 14: Ensemble mean of the maximum distance (in km) for the threshold exceedance of 10mSv for the inhalation thyroid dose for the seven participants, 24 hours after the beginning of the release, and associated standard deviations.

Level of agreement for threshold exceedance

The level of agreement maps for two participants are shown for illustration in Figure 15, with the 10-members simulation (left) and with the additional source perturbations (right). For these two participants, the maximum distance of threshold exceedance is lower with the perturbed simulations (503 km for BfS and 482 km for Met Office) than without (542 km and 578 km respectively). Figure 15 clearly shows that, although the area of highest probabilities is much smaller, the contaminated surface above the 5th percentile is much larger with the perturbed simulations. When taking into account different release times, different plume directions are taken into account (as shown by the trajectories Figure 4), which leads to a larger spread. Therefore, it is important to highlight that the maximum distance of threshold exceedance in itself is not a good indicator of the uncertainty: if the uncertainties are very large, then few members will agree with each other, leading to small probabilities and therefore, smaller distances. It should be associated with a map, in order to infer the possible contaminated areas, including those concerned by a low percentile.

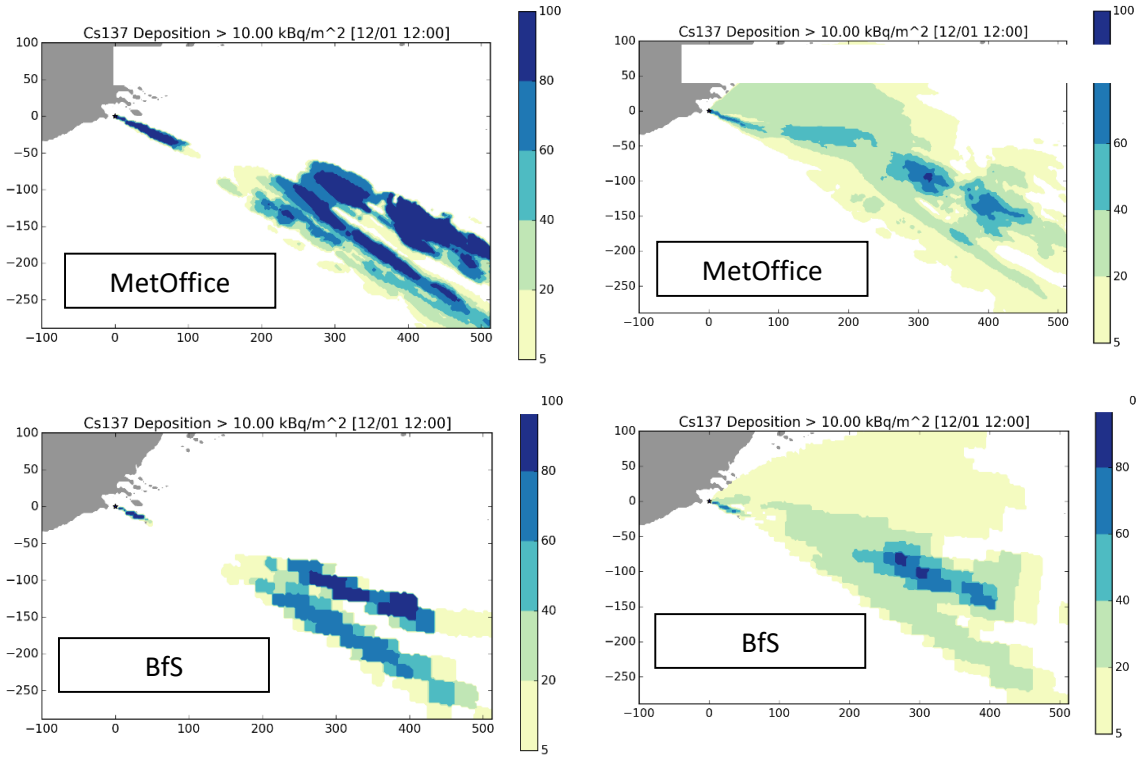

Figure 15 : Probability maps of a threshold exceedance of 10 kBq/m² for Cs-137 deposition, for a number of discrete bands of percentiles, without (left) and with (right) additional perturbations on the source term combined with the application of a meteorological ensemble.

In the remaining part of this chapter, only the results for the "full" ensembles, including source term uncertainties, are shown.

The levels of agreement of threshold of exceedance can be drawn for each ensemble, given an output variable and a threshold (Figure 16 and Figure 17). In Figure 16, the variability between the deposits of ^{137}Cs given by the participants is clear. It should be noted that, in this case, DTU did not perturb the release time; only the quantities were perturbed afterwards (Table 6), which explains the small area covered by the non-zero probabilities. All other participants show some probability of contamination in the north-eastern direction, due to a change in the release time. The pattern induced by scavenging, showing "hot spots" of deposition, is clear for most participants. Figure 17, representing the threshold exceedance of 10 mSv thyroid dose, shows a more continuous plume but still a large variability between the participants.

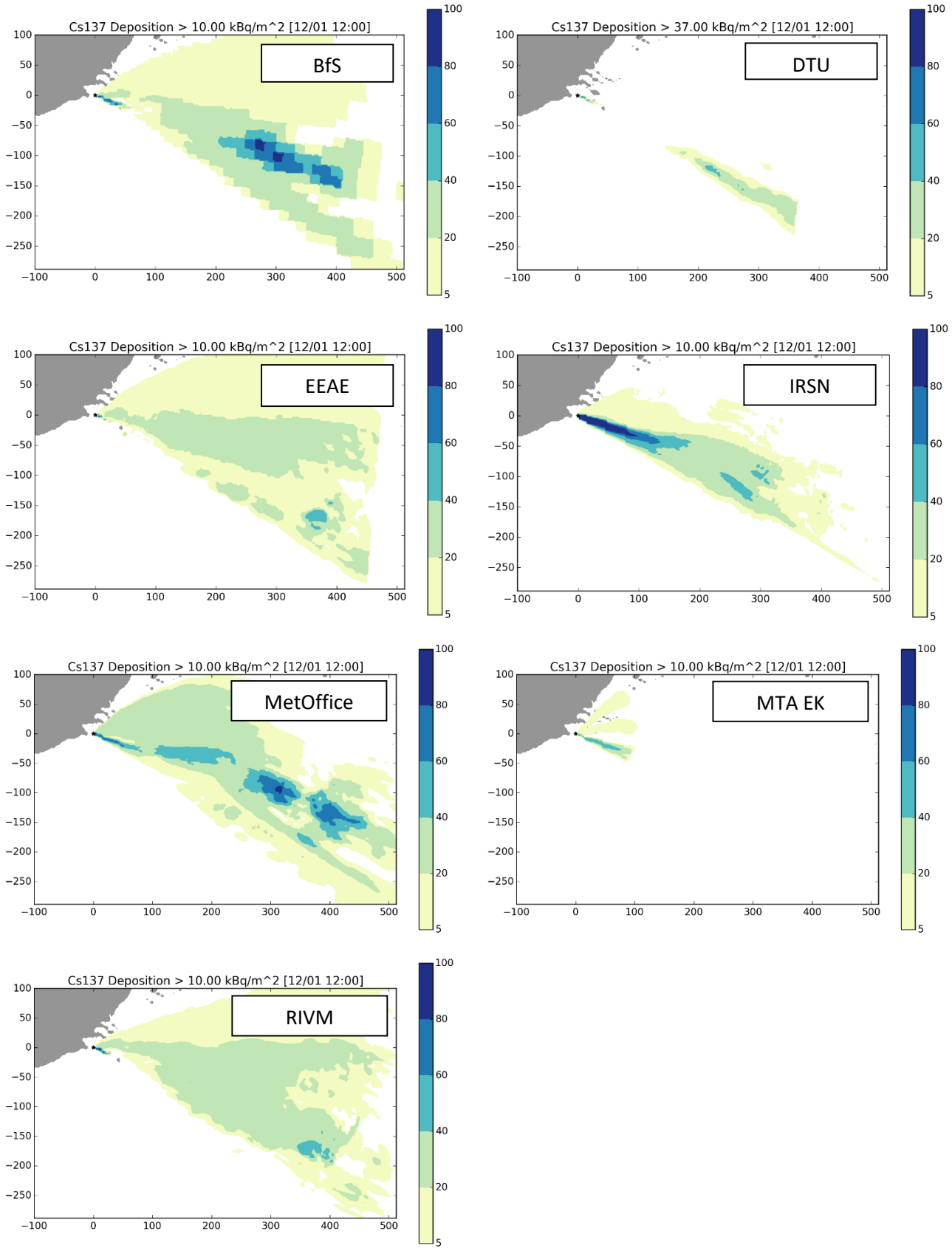

Figure 16 : Probability maps of a threshold exceedance of 10 kBq/m² for Cs-137 deposition, for a number of discrete bands of percentiles, for several participants.

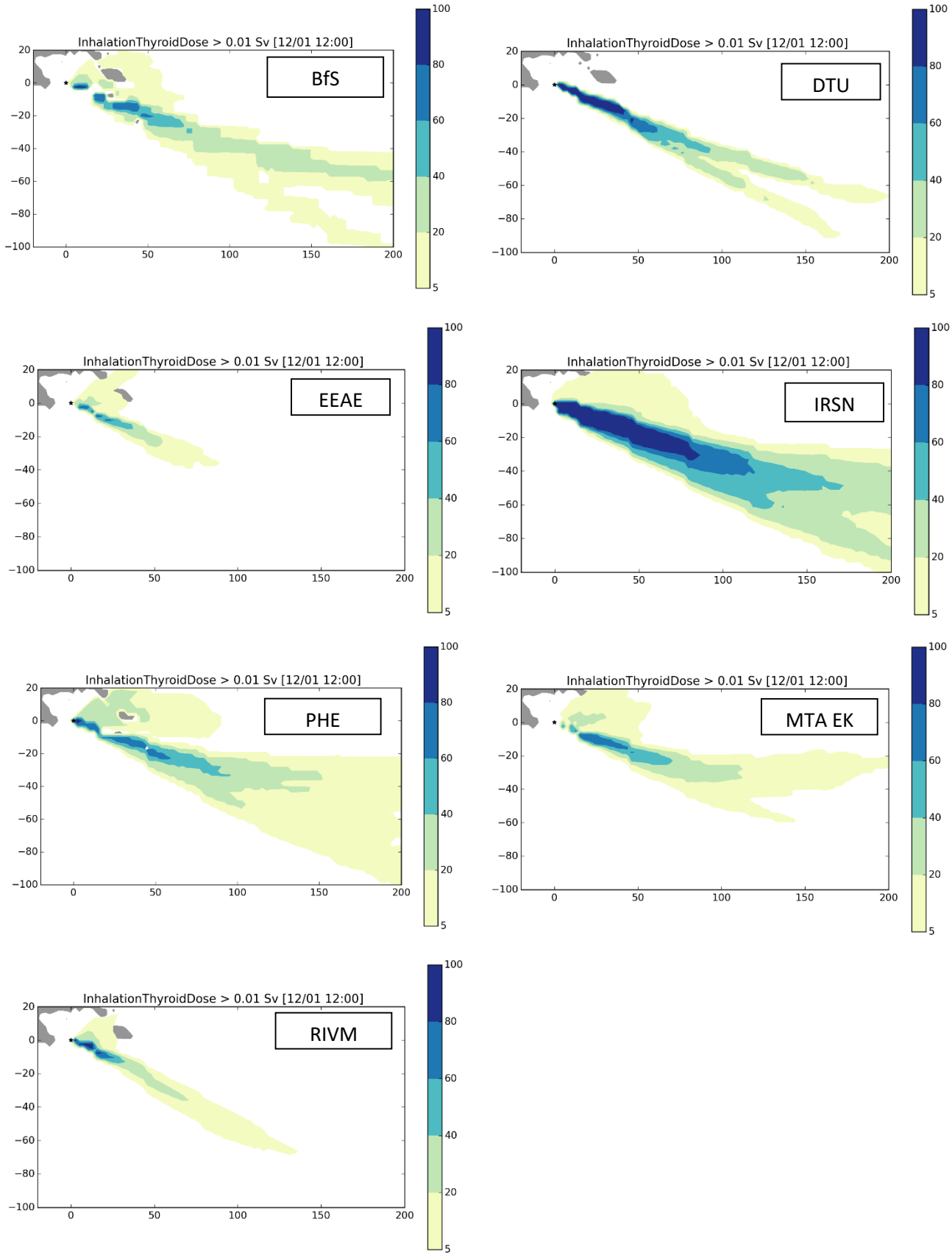

Figure 17 : Probability maps of a threshold exceedance of 10mSv for the inhalation thyroid dose, for a number of discrete bands of percentiles, for several participants, for the REM case study (short release) with source term perturbation and several variables of interest.

Ensemble results for REM2 – short release

This section briefly presents the results for the REM2-S case, corresponding to a release on January 12, at 18:00 UTC, with the same uncertainties on the release time, height and quantities as for the REM1-S case (provided in Table 6). Except Figure 18, both meteorological and source term uncertainties are taken into account. Figure 18 illustrates the inter-model variability by eliminating the differences in the source term perturbations between the participants: only the 10 meteorological members are used with the unperturbed source term. Therefore, all ensembles on this figure use strictly the same input data.

The median of the ensembles show that the deposition is globally higher close to the source than for REM1-S (Figure 18), which is explained by the presence of precipitation at the source location during the release time (Figure 6).The median plume trajectory is heading South-East and turning more East as the plume travels; the fact that some meteorological members may include trajectories heading North-East (Figure 9) is not reflected by the median maps. As for the REM1-S case, the median shows significant differences in the deposition between the participants. Beside interpolation and domain size artefacts, the plume spread is quite different, probably illustrating the variability between diffusion schemes. Again, wet diffusion schemes may explain some of the variability in the deposited amount of ^{137}Cs.

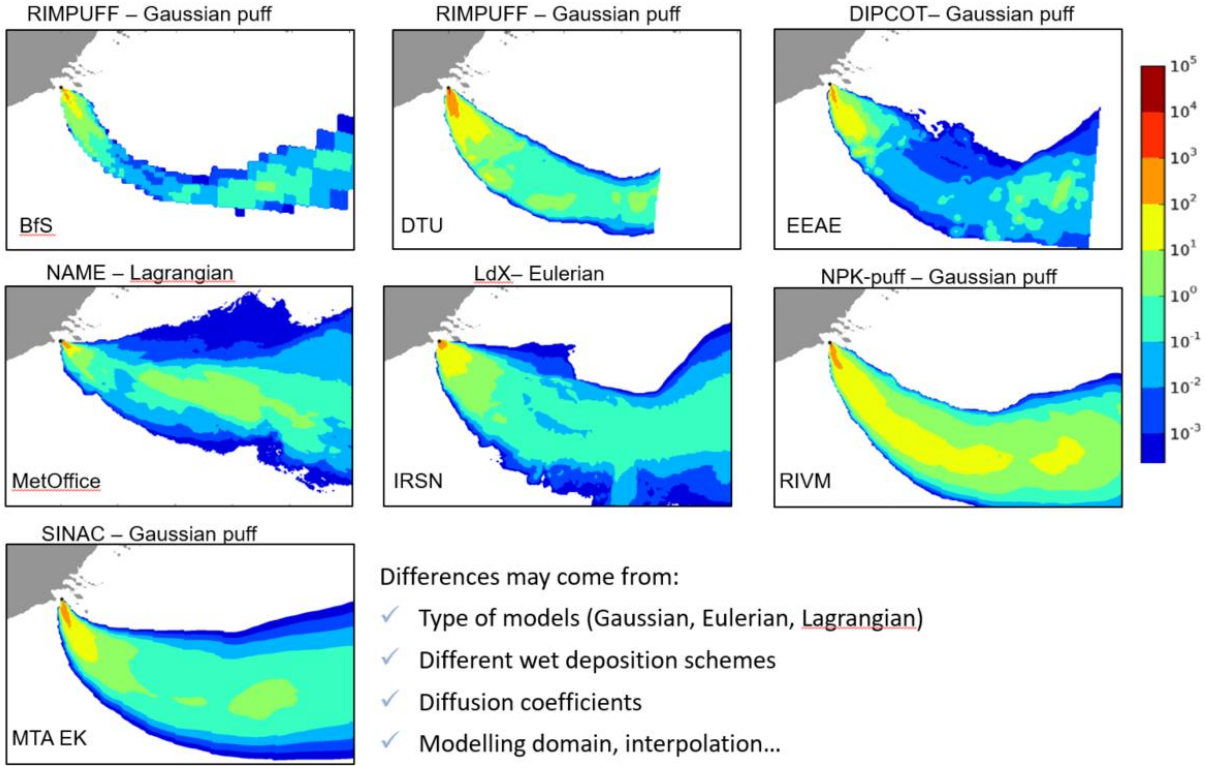

Figure 18 : median of the ^{137}Cs deposition in Bq/m^2 at the end of the release, for the seven ensembles. Only the meteorological uncertainties are taken into account (meteorological ensemble + reference source term without perturbation). Therefore, only the dispersion models differ between the participants. REM2-S case study.

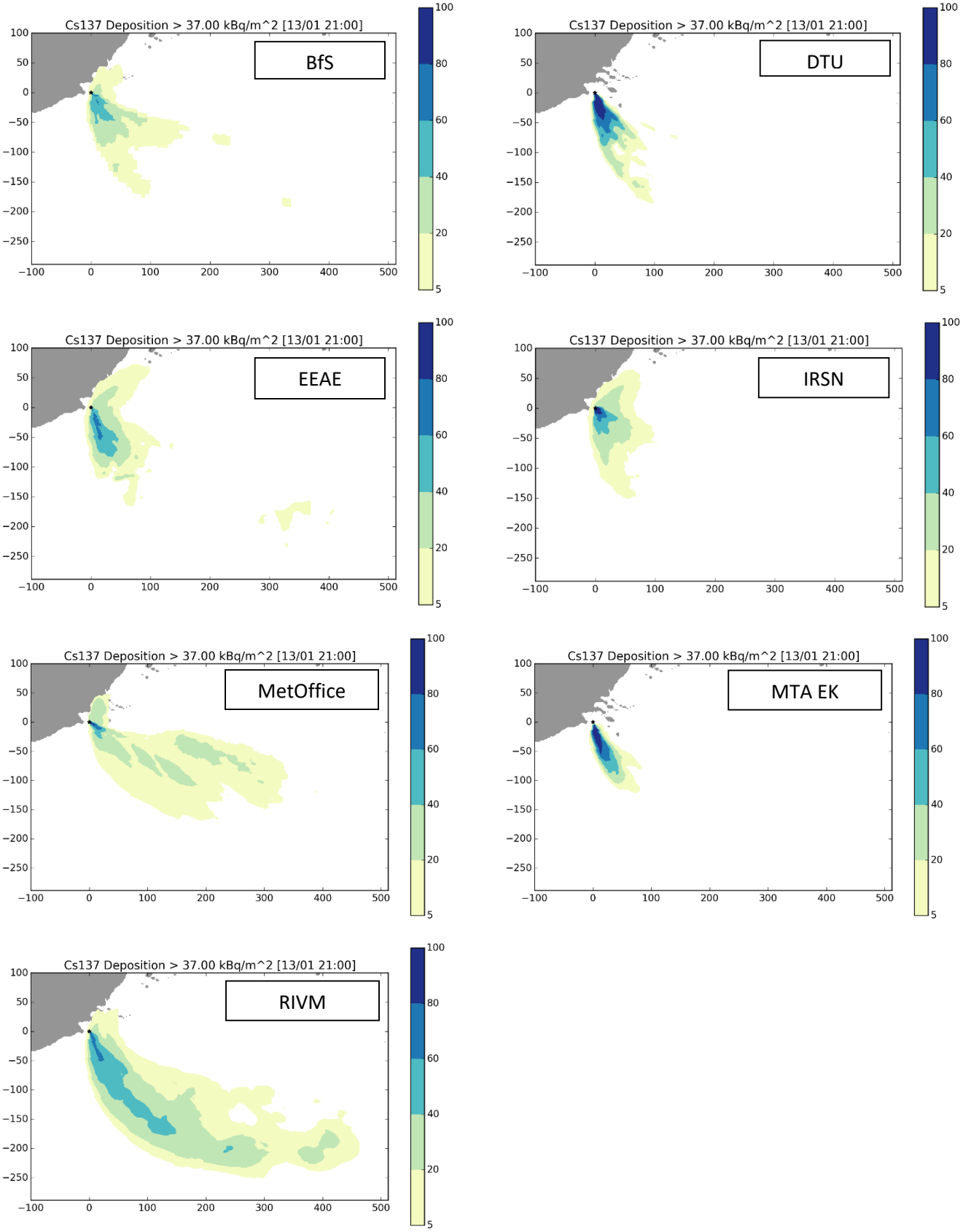

Figure 19 : Probability maps of a threshold exceedance of 37 kBq/m² for Cs-137 deposition, for a number of discrete bands of percentiles, for several participants. REM2 case study, short release.

The probability maps shown Figure 19 take into account both meteorological and source term variability. Here again, there are significant differences between the participants. In this case, in addition to the inter-model variability shown by Figure 18, they may also be caused by the various ways the source term uncertainties are taken into account. From the previous analysis of trajectories the plume may travel North according to several members; this is visible for several participants with a small lobe (low percentile) in this direction. In fact, precipitation exceeds 2mm/hr for many ensemble members and peaks as the wind direction changes between 18:00 UTC and 20:00 UTC (Figure 20).Thus, when the plume travels in that direction, the precipitation is so high that the plume is completely washed out before it has travelled very far, which explains the small distance of threshold exceedance.

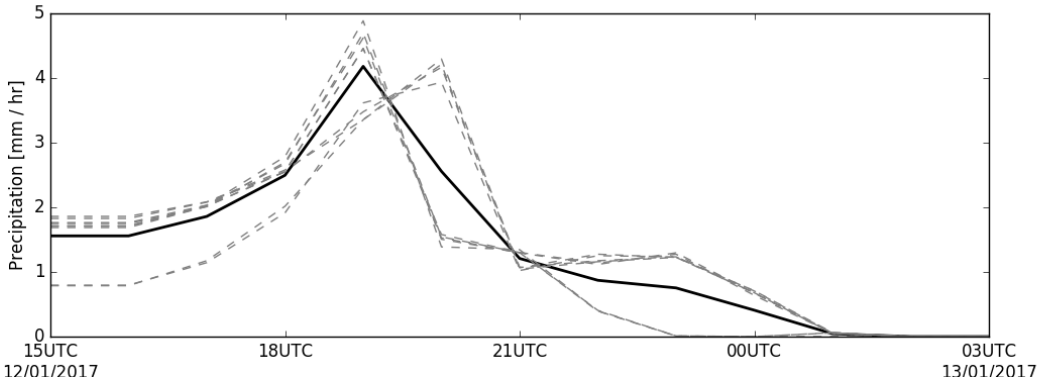

Figure 20 : precipitation (in mm/hr) as a function of time at the source location for the different ensemble members.

This variability in the areas affected by the contamination is not totally reflected when considering the maximum distance of threshold exceedance only (Figure 21(a)), which shows globally good consistency between the participants, both in the median and spread, except Met Office and RIVM which overestimate the deposition compared to other participants. The distances are globally lower than in the REM1-S case, which may be due to large precipitation close to the source, as mentioned earlier, as well as a convective situation favouring rapid mixing of the pollutants. As far as effective and inhalation thyroid dose are concerned, (Figure 21(b) and (c)), there is also globally a good consistency between the participants, when looking at the 25-75th percentile range; however, there are outliers (represented by blue crosses on the figures) for some ensembles, notably RIVM and BfS, which correspond to much larger distances of threshold exceedance: while the average distances for 10 mSv effective dose is below 20 kilometres, some particular members of these ensembles predict a threshold exceedance as far as 80 kilometres or more. This raises the issue of taking into account “extreme” values in case of emergency. In practice, such uncertainty assessment might be used for decision making as a way to prioritize the countermeasures, based on the probabilities associated with a given area. Countermeasures might be ordered in high-probability areas, and prepared in low-probability ones while waiting for more precise evaluations. Indeed, the uncertainties provided here are representative of the state of knowledge at a given time (in particular, uncertainty in the release time is still high) and may be reduced as the accidental sequence progresses (Figure 10). Finally, in Figure 21, IRSN presents two sets of results: those named simply “IRSN” represent cross-simulations, using only source term and meteorological perturbations, while “IRSN_MC” stands for “IRSN Monte Carlo” and represent the Monte Carlo ensemble designed as described in Table 7. The difference between the two results is therefore representative of the uncertainty related to physical parameters (diffusion and deposition). It does enhance a little the ensemble’s spread, particularly in the case of effective and inhalation dose; however, this is clearly of second order compared to meteorological and source term uncertainties.

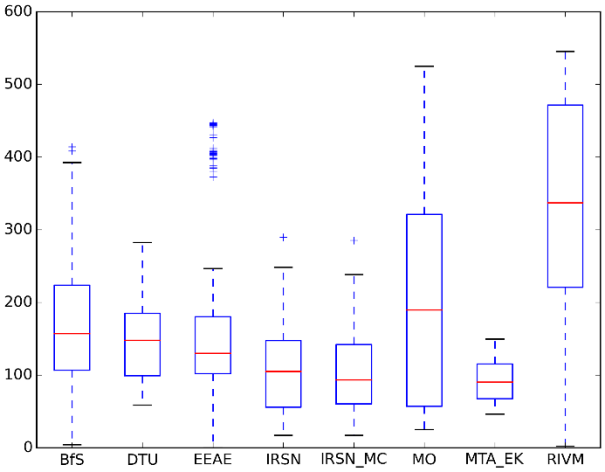

(a) Maximum distance of threshold exceedance of ^{137}Cs deposition for a level of 37 kBq/m^2

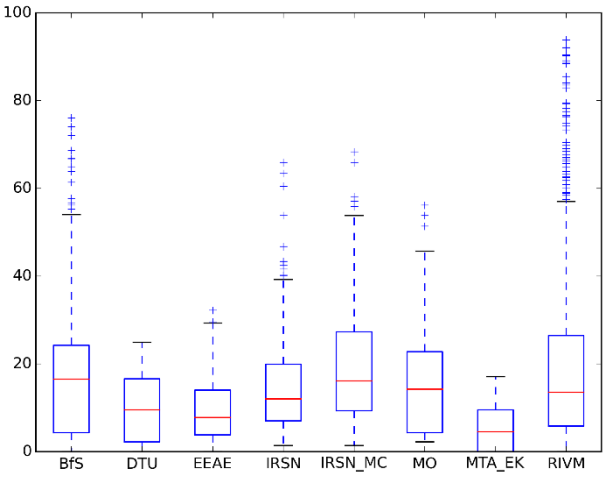

(b) Maximum distance of threshold exceedance of effective dose for a level of 10 mSv

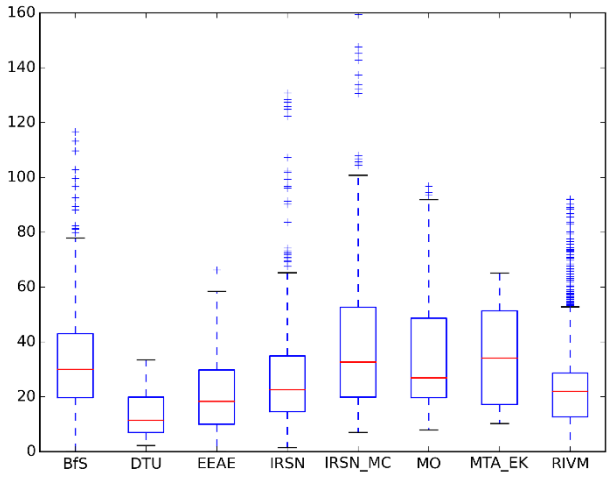

(c) Maximum distance of threshold exceedance of inhalation thyroid dose for a level of 50 mSv

Figure 21: Ensemble mean of the maximum distance for the threshold exceedance of (a) 37 kBq/m² of ^{137}Cs deposition, (b) 10 mSv for effective dose and (c) 50 mSv for inhalation thyroid dose, for the seven participants, 24 hours after the beginning of the release, and associated standard deviations. REM2 case study, short release.

Ensemble results for REM – long release

The long release begins on January 11th at 06:00 UTC and lasts three days. Therefore, it includes both weather situations described in the REM1 and REM2 scenarios. In particular, the time evolution of the release shown by Figure 11 indicates that there is a second, higher release for noble gas and gaseous Iodine (but not Caesium, as particles are filtered) corresponding to the opening of the containment venting system. There is a large uncertainty on the timing of this second release, but it occurs more or less 30 hours after the beginning of the release, which corresponds to January 12th at 12:00 UTC. Therefore, for a large part of the simulations, this second release corresponds to the REM2 situation described earlier in this report. Concerning the source terms, four participants (DTU, EEAE, IRSN and Met Office) used a reduced ensemble of ten source terms, designed to be representative of the original 150 ST ensemble's spread (as explained in (Bedwell et al. 2019), while the other two (BfS and MTA EK) used an ensemble of 5 source terms (designed in a similar way). Otherwise, inputs are the same (no additional perturbation for IRSN).Figure 22 features the probability maps associated with the REM-L simulations. There are, indeed, several areas potentially impacted by the plume, and in some cases, different "lobes" can be distinguished, indicating different plume directions. Here, only Iodine deposition is shown, as the release for Caesium was negligible due to the filtering, and no significant threshold exceedance could be displayed. The choice of using 5 source terms instead of 10 does not seem to be of primary importance for this kind of output: the map obtained by BfS (5 ST) is very similar, for instance, to that provided by DTU (10 ST), which is consistent with the fact that they use the same dispersion model (RIMPUFF). The results of those two participants were not so similar in the REM1-S and REM2-S cases, which was due to the difference in the way the two participants had perturbed the source term (Table 6). MTA EK have the highest deposition, which may partly due to the high scavenging coefficient, but also to other features related to dispersion, since inhalation thyroid dose is also very high (as can be seen on Figure 23(b)).Figure 23 shows the maximum distance of threshold exceedance for the different participants, for (a) a threshold of 10 kBq/m^2 for ^{131}I and (b) a threshold of 10 mSv for inhalation thyroid dose. While there is a significant variability in the ensembles' median, Figure 23(a) shows that there is a good consistency in the estimation of the overall uncertainty, represented by the blue boxes, between the participants, at least four of them (EEAE, IRSN, DTU and MetOffice).

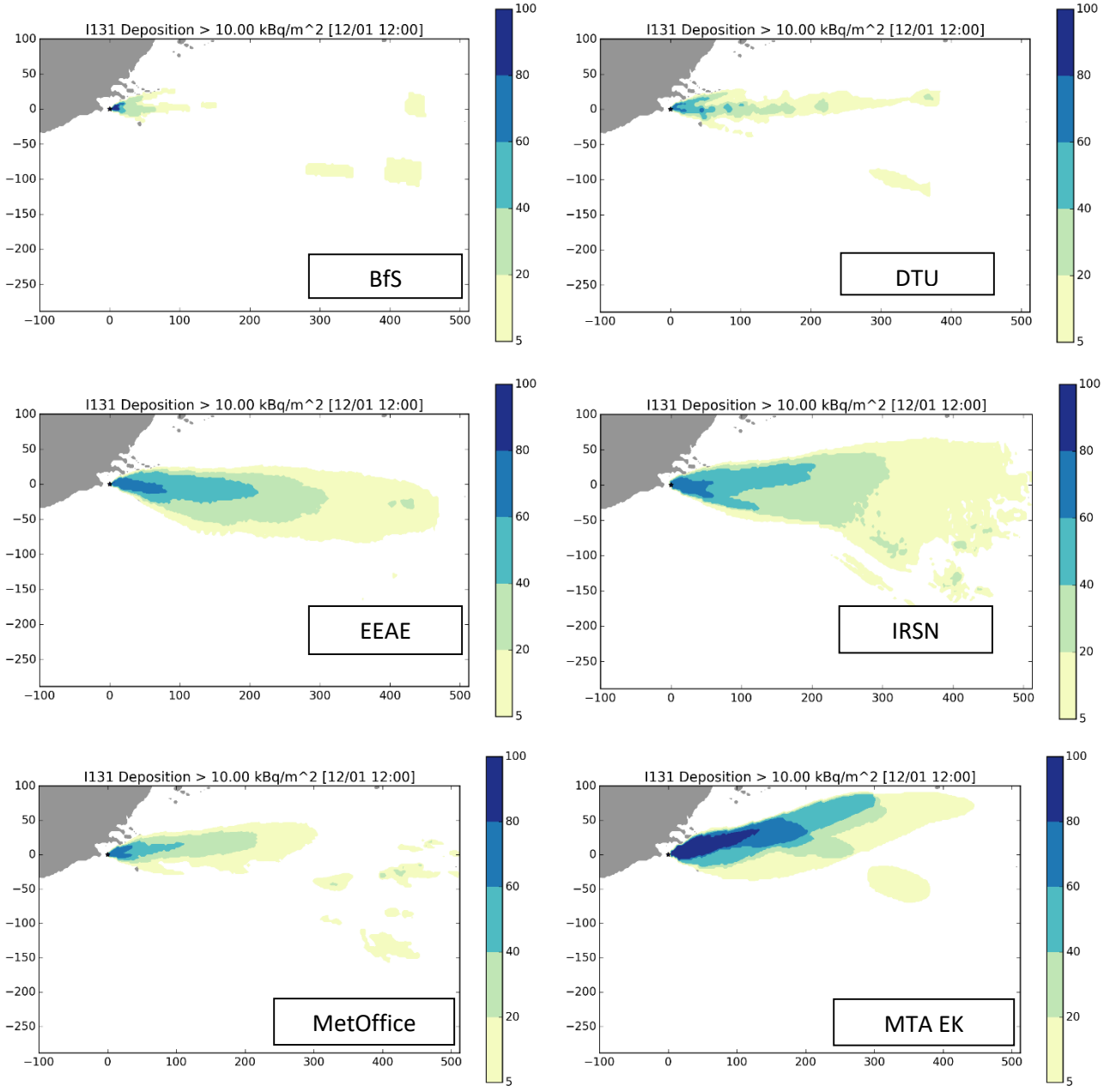

Figure 22: Probability maps of a threshold exceedance of 10 kBq/m² for I-131 deposition, for a number of discrete bands of percentiles, for several participants.

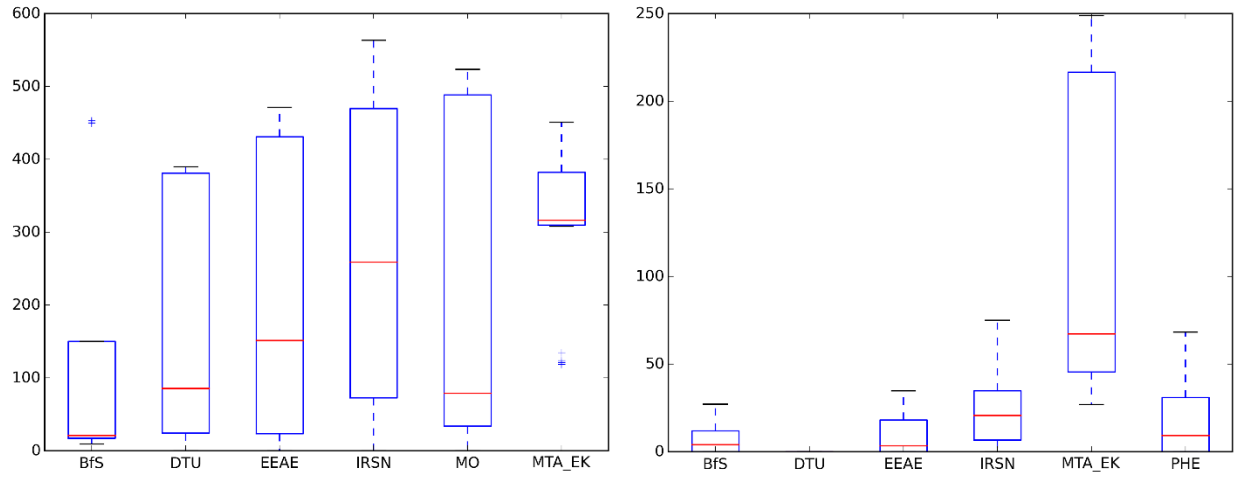

(a) Maximum distance of threshold exceedance of ^{131}I deposition for a level of 10 kBq/m^2

(d) Maximum distance of threshold exceedance of inhalation thyroid dose for a level of 10 mSv

Figure 23: Ensemble mean of the maximum distance for the threshold exceedance of (a) 10 kBq/m² of ^{131}I deposition, (b) 10 mSv for inhalation thyroid dose, for six participants, 24 hours after the beginning of the release, and associated standard deviations.

Conclusions

Three hypothetical accident scenarios that took place at Borssele (The Netherlands) have been investigated. They consisted of two different meteorological scenarios, REM1 with a small meteorological variability and REM2 with a larger variability, and two source term scenarios. The short release was used with both REM1 and REM2 scenarios, while the long release (3 days) covered both meteorological situations. This resulted in very large datasets (several hundreds of simulations carried out by six to seven participants for three cases). To our knowledge, this provides a unique database; usually, inter-comparisons such as the ones carried out here are focused on deterministic simulations.

For the two meteorological scenarios with the short release (REM1-S and REM2-S), seven participants carried out ensemble dispersion simulations, propagating both meteorological and source term uncertainties. Six participants provided results for the long release. Several endpoints were derived. A particular attention was devoted in this report to the maximum distance of threshold exceedance, for deposition, effective dose and inhalation thyroid dose. Several reference levels of interest for decision making were used. In addition to this variable, agreement maps were shown, that is, maps showing the proportion of ensemble members above a given threshold on each grid point.

The results showed that, when considering only meteorological uncertainty, there was a large variability in the outputs provided by the participants, especially when considering the maximum distance of threshold exceedance. In this case, the inter-model variability was clearly larger than the uncertainty linked to meteorological data (especially for the REM1 case). However, when considering source term uncertainties along with meteorological ensemble, the variability between the participants was of less importance, although not negligible. In particular, when considering exactly the same source term perturbations (for the long release), there was a good consistency between the participants' uncertainty estimates; the ensembles' spread mostly encompass the inter-model variability. These findings highlight the importance of properly taking into account all primary sources of uncertainties, especially the source term uncertainties and not only those stemming from the meteorological forecasts.

Another finding of this study was the sensitivity of the maximum distance of threshold exceedance to the input uncertainties. When more uncertainties are taken into account, the maximum distance (averaged

over the ensemble) tends to be reduced. In other words, if the uncertainties are large, ensembles' members tend to be in less good agreement with each other. This results in a larger surface covered by "low agreement" (e.g. 5th percentile) but numerical indicators averaged over the ensemble, such as the maximum distance of threshold exceedance, tend to be reduced. Therefore, care should be taken to not only use such a numerical output, but to include graphical representation of the uncertainties as well, such as the agreement maps (or maps provided for different percentiles), and/or maps given by one or several well-chosen members. The choice of the appropriate threshold, although usually driven by decision making, should also be made with care, as the outputs may highly differ depending on the threshold.

References

Baklanov, A. and J. H. Sørensen (2001). "Parameterization of radionuclide deposition in atmospheric long-range transport modelling." Phys. Chem. Earth (B) **26**(10): 787-799.

Bedwell, P., I. Korsakissok, S. Leadbetter, R. Périllat, C. Rudas, J. Tomas and J. Wellings (2019). D 9.5.5 Guidelines for the use of ensembles in the description of uncertainty in atmospheric dispersion modelling: operational applications in the context of an emergency response. D9.5 Guidelines for the use of ensemble calculations in an operational context, indicators to assess the quality of uncertainty modeling and ensemble calculations, and tools for ensemble calculation for use in emergency response, European Joint Program for the Integration of Radiation Protection Research CONCERT - CONFIDENCE project.

Bedwell, P., S. Leadbetter, J. Tomas, S. Andronopoulos, I. Korsakissok, R. Périllat, A. Mathieu, G. Geertsema, H. Klein, H. De Vries, T. Hamburger, T. Pazmandi, C. Rudas and A. Sogachev (2018). D 1.1.4 Guidelines detailing the range and distribution of atmospheric dispersion model input parameter uncertainties. D9.1 Guidelines ranking uncertainties for atmospheric dispersion, European Joint Program for the Integration of Radiation Protection Research CONCERT - CONFIDENCE project.

Bengtsson, L., U. Andrae, T. Aspelien, Y. Batrak, J. Calvo, W. d. Rooy, E. Gleeson, B. Hansen-Sass, M. Homleid, M. Hortal, K.-I. Ivarsson, G. Lenderink, S. Niemelä, K. P. Nielsen, J. Onvlee, L. Rontu, P. Samuelsson, D. S. Muñoz, A. Subias, S. Tijm, V. Toll, X. Yang and M. Ø. Køltzow (2017). "The HARMONIE–AROME Model Configuration in the ALADIN–HIRLAM NWP System." Monthly Weather Review **145**(5): 1919-1935.

Berge, E., H. Klein, M. Ulimoen, S. Andronopoulos, O. C. Lind, B. Salbu and N. Syed (2019). D 9.5.2 Ensemble calculations for the atmospheric dispersion of radionuclides. Hypothetical accident scenarios in Europe: the Western Norway case study. D9.5 Guidelines for the use of ensemble calculations in an operational context, indicators to assess the quality of uncertainty modeling and ensemble calculations, and tools for ensemble calculation for use in emergency response, European Joint Program for the Integration of Radiation Protection Research CONCERT - CONFIDENCE project.

Chevalier-Jabet, K. (2019a). Design and use of Bayesian networks for the diagnosis/prognosis of severe nuclear accidents, EU program for research and innovation H2020 - FAST Nuclear Emergency Tools (FASTNET) project. Report FASTNET-DATA-D2.3.

Chevalier-Jabet, K. (2019b). Source term prediction in case of a severe nuclear accident. 5th NERIS workshop. Roskilde, Denmark.

De Vries, H., G. Geertsema, I. Korsakissok, R. Périllat, J. Tomas, R. Scheele, S. Andronopoulos, P. Astrup, P. Bedwell, T. Charnock, T. Hamburger, I. Ievdin, S. Leadbetter, T. Pazmandi, C. Rudas, A. Sogachev, P. Szanto and J. Wellings (2019). D9.4 Published sets of probability maps of threshold exceedance for scenarios, European Joint Program for the Integration of Radiation Protection Research CONCERT - CONFIDENCE project. Report D9.4 20. http://www.concert-h2020.eu/en/Publications

Geertsema, G., H. De Vries and R. Sheele (2019). High resolution meteorological ensemble data for CONFIDENCE research on uncertainties in atmospheric dispersion in the (pre-)release phase of a nuclear accident. 19th international conference on Harmonisation within Atmospheric Dispersion Modelling for Regulatory Purposes, Bruges, Belgium.

IAEA (2011). Criteria for use in preparedness and response for a nuclear or radiological emergency: general safety guide. IAEA safety standards series No. GSG-2. Vienna, Austria, Jointly sponsored by the FAO, IAEA, ILO, PAHO, WHO. **STI/PUB/1467**.

Korsakissok, I., S. Andronopoulos, P. Astrup, P. Bedwell, K. Chevalier-Jabet, H. De Vries, G. Geertsema, F. Gering, T. Hamburger, H. Klein, S. Leadbetter, A. Mathieu, T. Pazmandi, R. Périllat, C. Rudas, A. Sogachev, P. Szanto, J. Tomas, C. Twenhöfel and J. Wellings (2019). Comparison of ensembles of atmospheric dispersion simulations: lessons learnt from the confidence project about uncertainty quantification. 19th international conference on Harmonisation within Atmospheric Dispersion Modelling for Regulatory Purposes, Bruges, Belgium.

Mathieu, A., I. Korsakissok, R. Périllat, K. Chevalier-Jabet, F. Stephani, S. Fougerolle, V. Créach, E. Cogez and P. Bedwell (2018). D 1.1.3 Guidelines describing source term uncertainties. D9.1 Guidelines ranking uncertainties for atmospheric dispersion, European Joint Program for the Integration of Radiation Protection Research CONCERT - CONFIDENCE project.

Périllat, R., I. Korsakissok, V. Mallet, A. Mathieu, T. Sekiyama, M. Kajino, K. Adachi, Y. Igarashi and D. Didier (2017). Using meteorological ensembles for atmospheric dispersion modelling of the Fukushima nuclear accident. 18th International Conference on Harmonisation within Atmospheric Dispersion Modelling for Regulatory Purposes. Bologna, Italy.

Saunier, O., A. Mathieu, D. Didier, M. Tombette, D. Quélo, V. Winiarek and M. Bocquet (2013). "An inverse modeling method to assess the source term of the Fukushima nuclear power plant accident using gamma dose rate observations." Atmos. Chem. Phys. Discuss. **13**(6): 15567-15614.